1-1-2019

Proactive Monitoring, Anomaly Detection, and Forecasting of Solar Photovoltaic Systems Using Artificial Neural Networks

Ahmad Almadhor
University of Denver

Proactive Monitoring, Anomaly Detection, and Forecasting of Solar Photovoltaic Systems Using Artificial Neural Networks

Abstract

The world of energy sustainability landscape is witnessing high proliferation of smartgrids and microgrids, it has become significant to use intelligent tools to design, operate and maintain such crucial systems in our lives. Solar energy is an intermittent source and purely Photovoltaic (PV) based, or PV and storage based smartgrids require characterization and modelling of PV resources for an effective planning and effective operations. This dissertation familiarizes briefly the existing tools for design, monitoring, forecasting and operation of a solar system in smart electric grids infrastructure and proposes a unique application-based infrastructure to monitor, operate, forecast and troubleshoot a working PV of a smartgrid. A resilient smartgrid communication is proposed which enables monitoring and control of different elements in any PV system. This communication architecture is used to facilitate a feedback-oriented monitoring of different elements in a microgrid ecosystem and investigated thoroughly. This integrated architecture which is a combination of sensors, network elements, database and computation elements is designed specifically for solar photovoltaic (PV) powered grids on modular basis. Apart from this, the network resilience and redundancy for smooth and loss less communication is another characteristic factor in this research work.

Subsequently, a deep neural network algorithm is developed to diagnose the underperformance in the generation of a PV system connected to a smartgrid. As PV generation is predominantly dependent on climatic parameters, it is necessary to have a mechanism for understanding and diagnosing performance of the system at any given instance. To address this challenge, this deep neural network architecture is presented for instantaneous performance diagnosis. The proposed architecture enabled modeling and diagnose of soiling and partial shade conditions prevalent with an accuracy of 90+%. Features of monitoring and regulating the generation and demand side of the grid were integrated through network along with feedback-based measures for effective performance in the PV system of a smartgrid or microgrid using the same network. The novelty in this work lies in real-time calculation of ideal performance and comparison for diagnosing critical performance issues of solar power generation like soiling and partial shading.

Furthermore, long-short term memory (LSTM), which is a recurrent neural network model, is created for forecasting the PV solar resources, in which can assist in quantifying PV generation in various time intervals (hourly, daily, weekly). PV based smartgrids often experience expensive or inaccurate resources planning due to the lack of accurate forecasting tools where the projected methodology would eliminate such losses.

This research work in its whole provides a different proposition of vertical integration which can transform into a new concept called Internet of Microgrid (IoMG). Planning, monitoring and operation form the core of smartgrids administration and if intelligent tools intertwined with network are being used as integral part in each of these aspects, then it forms a holistic view of smartgrids.

Document Type

Dissertation

Degree Name

Ph.D.

Department

Electrical Engineering

PROACTIVE MONITORING, ANOMALY DETECTION AND FORECASTING OF SOLAR PHOTOVOLTAIC SYSTEMS USING ARTIFICIAL NEURAL NETWORKS

_____

A Dissertation

Presented to

the Faculty of the Daniel Felix Ritchie School of Engineering and

Computer Science

University of Denver

_____

In Partial Fulfillment

of the Requirements for the Degree

Doctor of Philosophy

_____

by

Ahmad Almadhor

November 2019

Advisor: Dr. Mohammad Matin

Author: Ahmad Almadhor
Title: PROACTIVE MONITORING, ANOMALY DETECTION AND FORECASTING OF SOLAR PHOTOVOLTAIC SYSTEMS USING ARTIFICIAL NEURAL NETWORKS
Advisor: Dr. Mohammad Matin
Degree Date: November 2019

ABSTRACT

The world of energy sustainability landscape is witnessing high proliferation of smartgrids and microgrids, it has become significant to use intelligent tools to design, operate and maintain such crucial systems in our lives. Solar energy is an intermittent source and purely Photovoltaic (PV) based, or PV and storage based smartgrids require characterization and modelling of PV resources for an effective planning and effective operations. This dissertation familiarizes briefly the existing tools for design, monitoring, forecasting and operation of a solar system in smart electric grids infrastructure and proposes a unique application-based infrastructure to monitor, operate, forecast and troubleshoot a working PV of a smartgrid. A resilient smartgrid communication is proposed which enables monitoring and control of different elements in any PV system. This communication architecture is used to facilitate a feedback-oriented monitoring of different elements in a microgrid ecosystem and investigated thoroughly. This integrated architecture which is a combination of sensors, network elements, database and computation elements is designed specifically for solar photovoltaic (PV) powered grids on modular basis. Apart from this, the network resilience and redundancy for smooth and loss less communication is another characteristic factor in this research work.

Subsequently, a deep neural network algorithm is developed to diagnose the underperformance in the generation of a PV system connected to a smartgrid. As PV

generation is predominantly dependent on climatic parameters, it is necessary to have a mechanism for understanding and diagnosing performance of the system at any given instance. To address this challenge, this deep neural network architecture is presented for instantaneous performance diagnosis. The proposed architecture enabled modeling and diagnose of soiling and partial shade conditions prevalent with an accuracy of 90+%. Features of monitoring and regulating the generation and demand side of the grid were integrated through network along with feedback-based measures for effective performance in the PV system of a smartgrid or microgrid using the same network. The novelty in this work lies in real-time calculation of ideal performance and comparison for diagnosing critical performance issues of solar power generation like soiling and partial shading.

Furthermore, long-short term memory (LSTM), which is a recurrent neural network model, is created for forecasting the PV solar resources, in which can assist in quantifying PV generation in various time intervals (hourly, daily, weekly). PV based smartgrids often experience expensive or inaccurate resources planning due to the lack of accurate forecasting tools where the projected methodology would eliminate such losses.

This research work in its whole provides a different proposition of vertical integration which can transform into a new concept called Internet of Microgrid (IoMG). Planning, monitoring and operation form the core of smartgrids administration and if intelligent tools intertwined with network are being used as integral part in each of these aspects, then it forms a holistic view of smartgrids.

ACKNOWLEDGEMENTS

Words will not be enough to express how grateful I am to everyone who has helped me surpass my hard time being a student and a learner. Special thanks to my advisor Dr. Mohammad Matin and my co-advisor Dr. Jun Zhang, I will not forget the great help from my PhD supervisory committee members Dr. David Gao, ECE chair Dr. Amin Khodaei and Committee Chair Dr. Vijaya Narapareddy. Our Ritchie School of Engineering and Computer Science Dean JB Holston for his assistance and efforts, our amazing interim provost and Executive Vice Chancellor Dr. Corinne Lengsfeld for her support, Dr. Ann Petrila Assistant Dean GSSW and my generous sponsors Aljouf University.

My late great grandmother Ghuzayil Alkhaldi who passed away before seeing me graduating, grandmother Helalah Al-Ali, my mother Norah Alassaf, my father Saad Almadhor, my lovely daughters Norah and Maria, my siblings, I owe you everything in my life. My marvelous friends in the US, Saudi and all over the world, I'm grateful!

The DU family especially ISSS and LEP staff where I found peace and harmony working and assisting, Deborah Durkee, Kelly Parpovic, Director Lynne Warner, former Director David Gowdy and the rest.

Everyone in my life, THANK YOU

TABLE OF CONTENTS

LIST OF FIGURES

LIST OF TABLES

NOMENCLATURE

Chapter two:

P_{peak}	Peak power of the PV installation
G_{STC}	Solar Irradiance at Standard Test Condition (Usually 1000 W/m2)
T_{STC}	Ambient Temperature at Standard Test Condition (Usually 25 °C)
η_{Inv}	Inverter Efficiency
η_{Trans}	Transmission (Wire) Efficiency
α_T	Temperature co-efficient of PV module used for the installation
G	Function of irradiance
T	Function of Time
H	Length of day
φ	Latitude of a location
δ	Declination of the sun
N	Number of the day in a year
$E_{flow(t)}$	Energy flow at time (t)
$E_{PV(t)}$	Energy of PV
E_{Load}	Load demand of Energy
$P_t^{E,d}$	Power discharged by the battery bank to the load during time t
Δt	Time difference
η_d	Discharge efficiency
$P_t^{E,c}$	Power charged by PV into battery during t
Δt	Time difference

η_c	Charging Efficiency
$f_i(l)$	Flow in Channel i
N	Number of orthogonal channels
E	Number of data connections links
i	A channel
t	Time
l	Link
$\tau(l)$	Number of available channels for communications via link l
$\vartheta(l)$	Total number of available radio points for communications via link l
E	Number of data connection links at a particular node
α	A node
$C(a)$	A neighbor node (adjacent)
$S(a)$	A further away node
$u_i(l)$	Mean Utilization of channel
H	Total horizontal irradiance in Wh/m^2
G	Global radiation W/m^2
STC	Standard test conditions
Y_i	Ideal Performance (Ratio of H and G)
Y_r	Actual Yield
E_{pv}	Energy output of PV
P_{max}	Peak power of the system

$P.R.$ Performance ratio

E_{t+1} Energy of battery at time t+1

E_t Energy of battery at time t

P_t^c Power charged by the PV system into the battery bank during the time t.

P_t^d Power discharged by the battery bank to the load during the time t.

Δt Time difference

η_c Charging efficiency

η_d Discharge efficiency

$P^{c,max}$ Maximum Power that can be charged into the battery

$P^{c,min}$ Minimum Power that can be charged into the battery

$P^{d,min}$ Minimum power discharge that can occur in the battery

$P^{d,max}$ Maximum power discharge that can occur in the battery

ε Self-discharge energy loss of battery

$\delta_{c,t+1}$ Charge status of battery at time t+1

$\delta_{d,t+1}$ Discharge status of battery at time t+1

Chapter three:

V_{oc} Open circuit voltage

I_{sc} Short circuit current

P_{max} Maximum power

I Current

V	Voltage
I_L	Photo current
q	Charge
K	Boltzmann constant
A	Ideality factor of a p-n junction
I_p	Current of PV panel
n_p	Number of panels in array
I_r	Reverse saturation current
T_c	Cell temperature
T_{ref}	Reference temperature
E_g	Energy band gap of a solar cell
S	Irradiance
K_v	Voltage constant of cell
V_{pv}	Output voltage
P_{pv}	Power output of PV
E_w	Energy of wind
t	Time
Δt	Time difference
$\boldsymbol{\varepsilon_d}$	Discharge efficiency
P_{max}	Maximum discharging or charging rate of the battery
E_{max}	Maximum energy stored in the battery.
PT	Transmitting Data

s	Packet Size
d	Data rate
Ac	Energy Consumed by a node
C	A network node
N	Network
F	Function of the draining rate and available energy expressed
A_R	Residual available energy
R_D	Draining rate at a node
A_i	Initial energy
A_c	Current energy consumed at t for transmitting the data

Chapter four:

x_n	Irradiance value
$y_{t,m}$	Predicted solar data point sequence of values
λ	Activation function
W_{hx}	Weight matrix between hidden and input layers
W_{hh}	Recurrent weight matrix between the hidden and itself
b_h	Bias parameter for h
T	Transpose
W_{yh}	Weight matrix between hidden and output layers
b_y	Bias parameter for y
W	Weight Vector
μ	Average value

CHAPTER ONE: INTRODUCTION

1.1 Background and Literature

A microgrid in its true essence could be described as a miniature framework that has the capabilities to operate individually or can be synced with other grids. Microgrids are often viewed to be the best method for apprehending distributed generation as the evolving prospective system through a robust methodology in which deliberates connected loads and generation as a subsystem [1]. Smartgrids are usually seen as the best options for supplying rural areas since the transmission or interconnection with the main power grids is not possible or not practicable for various reasons. Until the dawn of renewable energy technologies in their current scale, conventional generation technologies such as gas, coal, etc. had shown dominance and had been favorable in supplying smartgrids with electricity. Nevertheless, the rapid advancing proficiencies in renewable resources generation, giving their tremendous advantages over conventional manners, has paved the way towards the incorporation of all available power resources into microgrids for noticeable commercial accomplishments [2]. Another advantage of intertwining renewable energy generation technologies with smartgrids is that they can benefit from the concept of enhanced reliability in active distribution by installing and positioning load centers nearby generation

with robust control and management systems. A comprehensive assessment of recent research accomplishments of smartgrid mechanisms along with all-purpose overview of the gains and characteristics of microgrids were introduced in [3]. In [4], connected and islanded assumptions in dc microgrid were studied along with their control and operation practices. In [5] and [6], cost optimization system and optimum operating stratagem were proposed for microgrids by using a fundamental approach. In recent times, amalgamation of islanded microgrids with solar photovoltaic (PV) power generation systems is motivating speedy development of distributed renewable energy systems, this would significantly enhance the affordability and accessibility of energy resources in rustic areas where lack of clean, efficient and dependable sources have been observed [7]. However, the main challenge associated with PV power generation is its intermittent nature which highly dictates its performance. Photovoltaic generation industry is going through a paradigm shift in terms of total renewable power generation and its related infrastructure. Furthermore, the twenty-first century is experiencing rapid technological development in numerous areas to facilitate sustainable living.

Exploiting the concept of Internet of Things (IoT), research on digital administration of powered smart and microgrids is gaining traction [8]. Artificial intelligence tools like Neural Networks are extensively being integrated with administration for applications such as real-time performance monitoring [9], diagnosis [10] as well as operations like load shedding [11].

A dedicated communication network is needed to monitor the performance of individual plant for sustainable operations and decision making in [12]. ANN based models widely expended for accurate power prediction and performance evaluation in these power plants. For example, the reports published by Solar Power Europe [13], emphasize the importance of ANN based tools to address the issues in renewable energy based powered smartgrids. Solar resources availability are circumscribed and in need of an precise modelling for power prediction, which includes climatic conditions similar to wind, temperature, irradiance, humidity and soiling. Research work reported in [14], predicted highest power harvest by implementing data input of weather elements into artificial neural networks techniques. In a similar research work described in [15], a proposal of radial basis function (RBF) was constructed neural network configuration to simulate PV solar arrays in a power plant. Experiments were carried out to predict solar radiation data using ANN models [16-20] to estimate power production of a PV system for a given duration. A day-ahead irradiance forecast was reported in [21] and [22], a comparison of different forecasting techniques was investigated in [23]. Artificial Neural Networks model was used in [26] and [27] to predict the power output of a PV system under dusty environmental conditions. Recent contributions use ANN models to achieve maximum power point (MPP) operations of a PV system [24], control and grid integration for residential solar PV operations [25] and adaptive ANN models for standalone PV systems [28]. Other applications of ANN models include health monitoring of PV arrays [29], hour ahead

forecast of energy price in industries [30] and fault diagnostics of multilevel inverter used in these power-generating plants [31] With the advent of fourth industrial revolution, the intersection of electrical and communication networks for monitoring and control of utility level infrastructure seems inevitable [32]. Researchers designed and developed communication architecture intertwined with PV generation systems for smartgrids [33], grid-connected PV plants [34] and distributed solar power generation systems [35]. In [12], a mesh network-based communication architecture is proposed to monitor and control different elements in a PV powered microgrid, Figure 1.1.

With the increase in the intensity of renewable proliferation and its injection into utility grid, monitoring the assets that produce the energy and continuously evaluating the parameters (climatic) that dictate the performance is becoming increasingly important [37]. Researchers predict the transformation of normal electric grids into smart, next generation electric grid with renewable generation sources that will inevitably have the intersection of electrical as well as communication systems [38].

The combination of electrical and communication systems, will enable functions based on the motivation of grid, like online monitoring, demand-side management, control along with critical functions like troubleshooting an event and its immediate reporting [39]. Sood et.al [40] developed a WiMax (Worldwide Interoperability for Microwave Access)-based smartgrid communication network for monitoring distributed energy generation sources. In a similar work [41], a grid-connect AC microgrid was simulated using the

Simulink tool with basic communication infrastructure and a control strategy to optimize the performance in the grid was discussed. Masud and Li [42] developed and analyzed Internet of Things (IoT) based communication network for monitoring multiple distributed energy sources using Kalman filter-based state estimation of the electric grid. In [43], an IoT-based energy management system in smartgrids for improving efficiency was proposed and studied in the context of PV generation systems, while a similar energy management system in a PV/wind hybrid smartgrid was simulated in [44] and [45] using Simulink. A Self-Sustaining Wireless Neighborhood Area Network was designed in [46] for transmitting power grid sensing and measuring status as well as the control messages. While Spano et.al [47] included individual energy meters into the communication network to design a holistic model for smartgrid monitoring. Kristensen et.al [48] developed information access schemes between remote assets and controller, which are activated only when certain voltage thresholds are at any measurement point in the grid.

Apart from monitoring, control is one of the important features that can be made possible through smartgrid when the right infrastructure is in place. Several models based on mathematical constraints of a practical grid in operation have been developed to control and optimize the performance of a smart and microgrids. Anderson et al. [49] demonstrated the concept of "gridcloud" comprising of a wide area architecture to monitor and control a smartgrid. A robust optimal control strategy for an energy storage system of a grid-connected microgrid is elaborated in [50]. For a PV-wind-diesel-battery hybrid system, Ai-

barazanchi and Vural [51] developed a control mechanism by controlling the Pulse Width Modulation (PWM) of Voltage Source Converter (VSC). Phung et.al [52] presented a dependable control using IoT backbone for administration of a smartgrid. Along similar lines, a holonic architecture is proposed in [53] and a Fuzzy based frequency control is discussed in [54] to address the challenges of operating grid comprising of wide variety of heterogeneous producers and consumers that are unpredictable. Design, control and performance evaluation of a hybrid microgrid comprising of solar and wind is proposed in [55] using principles of power electronic operations.

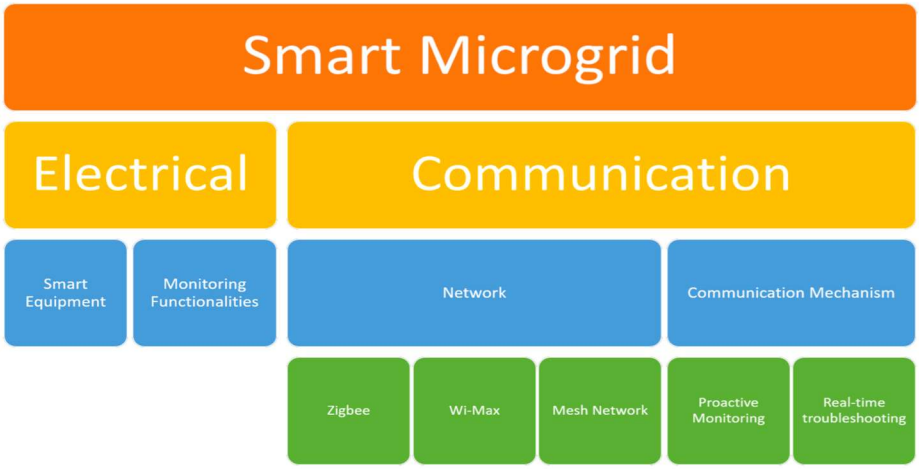

Figure 1.1 Intersection of Electrical and Communication Infrastructure - Root of Digitalization.

Since demand-side management forms a crucial part of any grid, Yang Mi et.al [56] studied a droop control-based power sharing mechanism in a microgrid and supported it through Simulink simulations. A voltage sensor combined with current estimation algorithms were proposed and discussed for load management in [57]. A game-theory-

based, flexible control of demand using proportional allocation was proposed in [58] for an autonomous grid operation. Emphasizing on the stability of smart grids Krisminato et al. [59] developed a comprehensive small-signal model of a hybrid renewable-energy-based microgrid to observe its performance. Since the smartgrids are vulnerable to cyber-attacks, it is equally important to consider the privacy and security aspects of the grid. There are established standards [60] along with case specific attack solving tools [61] to effectively address this aspect. Artificial Networks are one of the undoubtedly abundant schemes toward smarter renewable power grids with their capabilities to perform dynamically. Recurrent Neural Networks (RNN) have shown strong competences in precise for short-term learning rate and accurate forecasting models. Unambiguously Long-short term memory (LSTM) [82] has been evident in proving prolonged term memory as a special model of RNNs. However, Support Vector Machines (SVMs) [83] were popular in statistical classification of data but lack several recompenses when more advanced methods arisen. SVMs in its new form of Regression enthused models or as called Support Vector Regression (SVRs) models [83]. Such models would be a greatly contribution in providing sophisticated accuracy projection for the grids mechanisms particularly in islanded mode smart and microgrids. Solar forecasting techniques have been under focus in the recent years due to the proliferation of RESs more widely than ever which has generated numerous projects around the world [84]. Predicting and forecasting in the generation of renewable energy has voluminous approaches which are varied as

numerical, statistical, Artificial, Physical and others. In [85], the authors have proposed five classifying categories of forecasting as:

a) Artificial intelligence (AI)[86]-[87]: Deep Neural Networks (DNN), Artificial neural Networks (ANN), and K-Nearest Neighbors (KNN).

b) Regressive methods: Autoregressive integrated moving average (ARIMA), nonlinear stationary models and Autoregressive.

c) Hybrid Models[88]: Neuro Fuzzy systems and others.

d) Numerical Weather Predication (NWP)[89]: Grid points models and others.

e) Sensing as in [90] and [91].

In figure 1, the anatomy of the irradiance forecasting, and prediction methodologies are presented generally where much more can be found in depth, also relying techniques exist but those mentioned in the anatomy are generic. Physical systems are expensive to install, update or expand; thus, convoluted to recuperate. Statistical models have shown promising enhancements and encroachments; subsequently more accuracy, manipulating and implementation. Artificial Intelligence and machine learning prototypes explicitly Neural Networks (NN) are driving the forecasting enigma toward keener and more precise.

Support Vector Machine (SVM) technique is a machine learning statistical system wherein assisting in minimizing the structural risk [92]. The improved version of SVM which is Support Vector Regression (SVR), is structured to stretch the nonlinear input to a

wider dimensional chattels for the sake of finding the hyperplane in order to widen the margin of tolerance [92].

1.2 Problem Statement

With the advent of renewable energy-based electricity generation, the aspect of modelling and characterizing intermittency of these generation sources is increasingly gaining importance. This modelling can help in planning, performance evaluation, accurate forecasting, operation and maintenance of systems powered by renewable sources. Solar PV smartgrids are proliferating at high intensity across the globe. To ensure sustainable operation of such smart electric grids, it is absolutely necessary to characterize the performance and accurately forecasting to be in a position to point out underperformance, if any, in these PV systems of smart and microgrids. Deep and Recurrent artificial neural networks, one of the many tools of artificial intelligence is used to facilitate and achieve this characterization, thus performance evaluation and sophisticated accuracy forecasting.

1.3 Motivations

Given the rapid expansion of the fourth industrial revolution, the intersection of electrical and communication networks for monitoring and control of utility level infrastructure seems inevitable [94]. Researchers designed and developed communication architecture intertwined with PV generation systems as in smartgrids [95], grid-connected PV plants [96] and distributed solar power generation systems [97]. In [98], IEEE smartgrid

communication vision document outlines the necessity of communication intertwined with smartgrids in the following ways:

- Power entropy: Distributed and renewable generation in particular should remain synchronized with the main ac power frequency; maintaining frequency synchronization is a challenge requiring communication related to the inertia/momentum of the distributed/renewable generators. Figure 1.1 shows a simple communication network and equipment infrastructure for smartgrid technologies for renewable integration. In addition, power generation for renewables is subject to potentially high entropy weather variations whose communication requirements are proportional to the entropy.
- Power area or density (dispersal/aggregation): The area of power control can be from a large wind farm to the inverter control for a domestic photovoltaic system over a distribution system of today's power grid architecture.
- Power efficiency: Maintaining the power factor within tighter bounds will require more communication.
- Amount of power drives latency: As an example, protection mechanisms for distributed generation will require communication proportional to the amount of power similar to a time-current characteristic curve.

As the number of devices that participate in smart electric grids increases, the relevant smart operations are increasingly adopting a decentralized approach [99], rather

than a centralized one, leading to a subsequent increase in vulnerability and security risks of transmissions. To accomplish enhanced echelons of sanctuary, reliability and privacy, transmission schemes should be capable of detecting and handling eavesdroppers and malicious behavior [100]. The adopted schemes could utilize ideas from information theory (such as the notion of secrecy capacity [101]), multi-agent approaches [102] and game-theoretic modeling, while considering the constraints that are imposed, e.g, by critical smartgrid operations (e.g., power balance control) with low latency requirements. For energy management and demand response purposes, the power consumption signals of the domestic appliances of multiple houses are gathered at a remote concentration center for supporting decision making procedures [103]. The amount of data, however, could be excessive which could exhaust the available resources of the communication infrastructure, meaning that compression techniques should be employed. Sparse coding and dictionary learning algorithms [104] can lead to novel compression techniques, which are particularly suited to the considered consumption signals.

While taking cue from the IEEE vision document on smartgrids communications, this work aims at characterization and performance evaluation of a PV system for potential implementing in smartgrids through a dedicated architecture.

1.4 Objectives

- Familiarizing briefly the existing tools for design, monitoring, forecasting and operation of PV solar systems in smart and microgrids infrastructure.

- Proposing a unique application-based infrastructure to monitor, operate, forecast and troubleshoot a solar PV system in smart and microgrids.
- Insinuating a resilient solar smartgrid communication infrastructure in which enables monitoring and control of different elements in such power systems.
- Facilitating a feedback-oriented monitoring of different elements in the PV based smartgrid ecosystem.
- Identifying the reasons of underperformance in the PV based system using the communication infrastructure.
- Implementing and comparing various forecasting techniques for improved precision.
- Providing a unique proposition of vertical integration which can transform into a new concept called Internet of Microgrid (IoMG) where planning, monitoring, forecasting and operation form the core of smartgrid administration intertwined with network to form a holistic view of smartgrids.

1.5 Methodologies

- PV based microgrid system is simulated based on meteorological settings of a location and an ideal performance model is created [12].
- A communication system is designed to integrate elements of a smartgrid spread across an area [12].
- Real-time performance data is obtained through a projected communication infrastructure [12].

- Configuring a rule-base for identifying and characterizing the aspects of PV performance.
- Feedback-based monitoring to identify underperformance by comparing ideal value (generated through ANN) with real-time value. In the due course, the performance of network and battery are also monitored [12],[36].
- Dwelling down to granular level by developing models to identify the reason for underperformance [36].
- Collect data samples for PV performance while subjected to soiling and shading.
- Developing a DNN model to characterize the underperformance aspects and integrate it with ANN model for identifying the reasons for underperformance [36].
- Use real-time data through the developed model to identify whether a system is underperforming. If so, finding out the reasons for such underperformance [36].
- RNN Long-Short term memory (LSTM) is developed and simulated for forecasting and then comparing performance with conventional methodologies as Support Vector Machines-regression [91].

1.6 Dissertation Outline

The main aim of this research work is to streamline the monitoring, operation and forecasting of a PV powered electric grid (smart or microgrid) and generation systems using artificial intelligence techniques and mesh networks. In this regard, a suggested and investigated architecture for real-time monitoring for feedback-based decision making is proposed in chapter 2. This monitoring network is extended for diagnosing or

troubleshooting PV generation using a combination of deep neural networks and conventional neural networks as explained in chapter 3.

A recurrent neural network technique for irradiance and generated power forecasting using LSTM is proposed along with simulating SVR forecasting, a comparison study is achieved and explained in chapter 4 for short, medium and long terms.

CHAPTER TWO: FEEDBACK-ORIENTED INTELLIGENT MONITORING OF A STORAGE-BASED SOLAR PHOTOVOLTAIC (PV)-POWERED MICROGRID WITH MESH NETWORKS

2.1 Microgrid Architecture

A basic microgrid, as represented in Figure 2.1 is used for this research work. This microgrid consists of a solar power generation system with battery back-up. An inverter is represented after the DC bus bar, which supplies the AC power to the connected load.

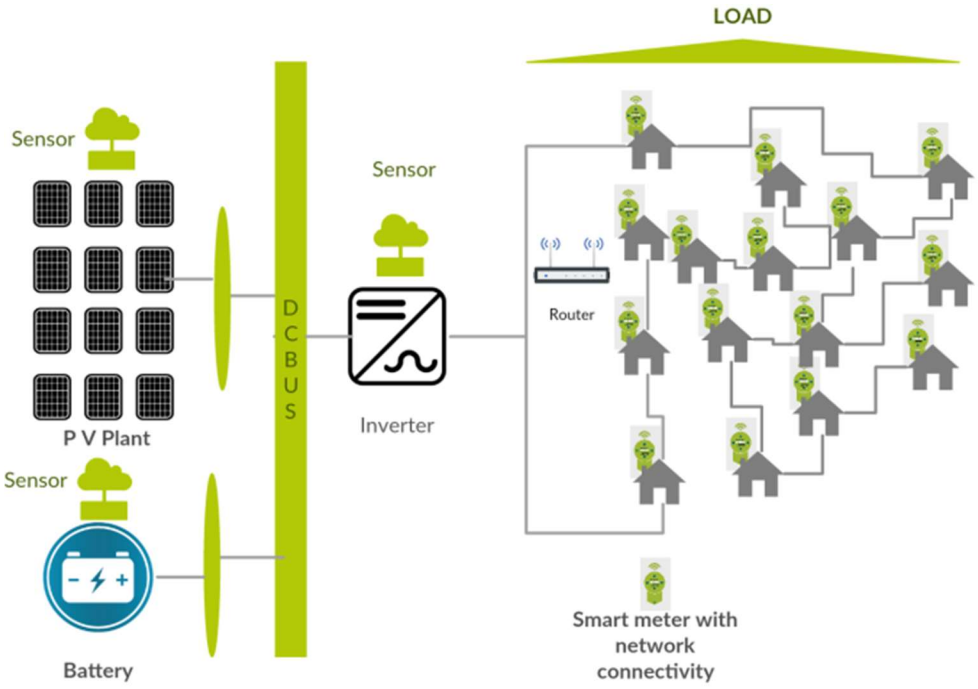

Figure 2.1 Microgrid electrical configuration overview.

In typical applications, microgrids are used to power rural areas without electricity access. Hence, load characteristics considered here are strictly in lieu with typical residential consumption profiles. The microgrid architecture illustrates sensors connected to each generation node, inverter and battery. This is to facilitate monitoring of generation, transmission and consumption where the houses are assumed to have smart meters installed.

2.1.1 Photovoltaic System

Photovoltaic generation is connected to the DC bus through a controller powered with Maximum Power Point Tracking (MPPT). The power output of a PV generation system can be mathematically expressed as a function of Irradiance (G), Temperature (T) at a time (t) [62] as:

$$P(t) = \left[P_{peak}\left(\frac{G(t)}{G_{STC}}\right) - \alpha_T(T_c(t) - T_{STC})\right] * \eta_{Inv} * \eta_{Trans} \quad (1)$$

where,

P_{peak}: Peak power of the PV installation

G_{STC}: Solar Irradiance at Standard Test Condition (Usually 1000 W/m2)

T_{STC}: Ambient Temperature at Standard Test Condition (Usually 25 °C)

η_{Inv}: Inverter Efficiency

η_{Trans}: Transmission (Wire) Efficiency

α_T: Temperature co-efficient of PV module used for the installation

There are different models to calculate the energy generated from a PV system at a given location. The widely-used expression talks about energy as a function of solar radiation data in terms of a time function for the total available day light hours on a given day. This can be mathematically expressed as:

$$E_{PV}(t) = P(t) * H \quad (2)$$

Where H is the length of the day and is represented as:

$$H = \frac{2}{15}\cos^{-1}(-\tan\varphi * \tan\delta) \quad (3)$$

Where φ is the Latitude of the location and,

$$\delta = 23.45 * \sin\left[\frac{360*(284+N)}{365}\right] \quad (4)$$

Where N is the number of the day in the year (For example, if it is June 21, N = 172).

2.1.2 Battery System

The priority in any battery connected PV system for energy flow is the load. Hence, the effective energy across the battery is always the difference between the consumption at the load and generation. This can be expressed as:

$$E_{flow(t)} = E_{PV(t)} - E_{Load(t)} \quad (5)$$

If $E_{Load} > E_{PV}$, there is deficit energy and battery is not charging

If $E_{PV} > E_{Load}$, there is excess energy and battery is charging

The discharge state on a battery at a given time t + 1 can be expressed as [63]:

$$E_{t+1} = E_t - \Delta t \frac{P_t^{E,d}}{\eta_d} \quad (6)$$

Where,

$P_t^{E,d}$ is the power discharged by the battery bank to the load during time t.

Δt is the time difference.

η_d is the discharge efficiency.

While the charging status at t+1 can be expressed as:

$$E_{t+1} = E_t + \Delta t * P_t^{E,c} * \eta_c \quad (7)$$

Where, $P_t^{E,c}$ is the power charged by the PV system into the battery bank during the time t.

Δt is the time difference,

η_c is the charging efficiency.

Hence, the energy flow in the battery can be represented as:

$$E_{t+1} = E_t * \eta_{Inv} * \eta_d * \eta_{Trans} + E_{flow(t)}\ ;\ \text{when}\ E_{flow(t)} < 0 \quad (8)$$

$$E_{t+1} = E_t * \eta_c - E_{flow(t)}\ ;\ \text{when}\ E_{flow(t)} > 0 \quad (9)$$

$$E_{t+1} = E_t\ ;\ \text{when}\ E_{flow(t)} = 0 \quad (10)$$

2.1.3 Load Profile

A load profile for 75 households is simulated based on the consumption of energy when using equipment like electric bulbs, fans and televisions. Figure 2.2 represents the daily average consumption of 75 households. This pattern is generated keeping in view the usage of electricity and appliances in rural areas which have no prior electricity access [64]. A rural area in the country of Guinea in Africa was used as an example in this research work. The load profile was created using the consumption metrics defined for any rural area in this country. The yearly average profile is illustrated in Figure 2.2.

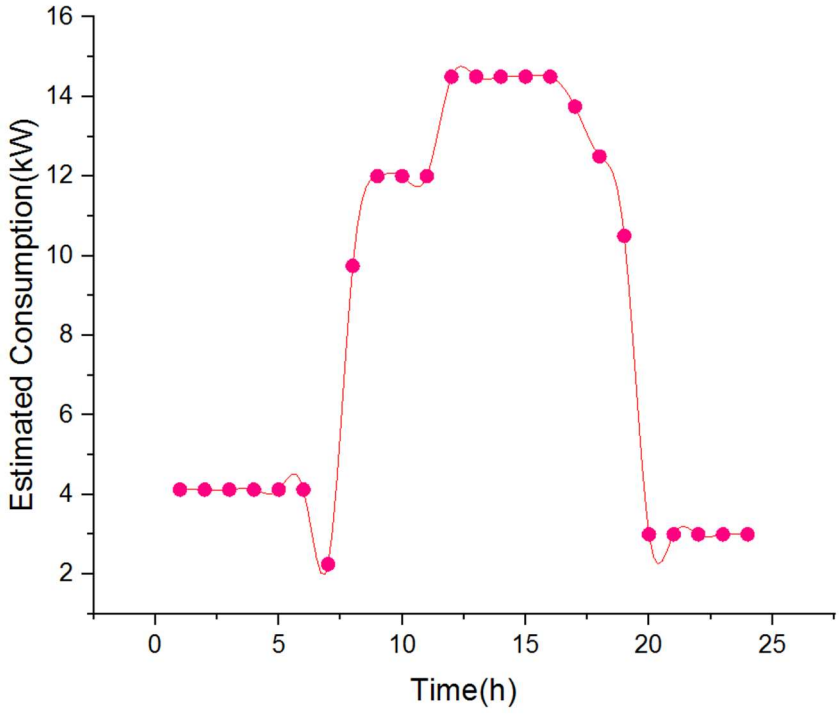

Figure 2.2 Simulated load profile for a rural area.

2.2 Microgrid Communication Architecture

A smartgrid communication is increasingly becoming multipurpose due to automation of aspects like demand-side management, generation management, load shedding (whenever necessary), event reporting and troubleshooting of malfunctioning equipment. There is a need for effective and sustainable communication architecture in a microgrid for the following reasons:

- **Intermittent nature**: Renewable energy sources, with the virtue of being dependent on natural elements, are known for their notorious intermittency. When the proliferation of renewable-energy-based smart and microgrids are increasing, there is a dire need in continuously monitoring the weather parameters, their influence on power generation and tune the system to adapt for extreme events.
- **Bi-directional flow:** With the advent of smartgrids, electricity consumers are no longer solely consumers but are slowly turning into prosumers (Producer + Consumer). Distributed rooftop installations and smart meters are paving the way to this revolution. Hence, an integrated communication architecture that can accommodate the requests from individual installations to grid and facilitate energy transfer in any direction is necessary to have integrated communication architecture.

Hence, in this research work, communication architecture is designed keeping in view the aspects by classifying the elements into clusters. Every cluster contains either of

generation or consumption elements intertwined with communication architecture and analytics functionalities. In this research work, there are two such clusters, one for generation and the other for consumption nodes. The functional overview of the communication network developed in this research work is illustrated in Figure 2.3.

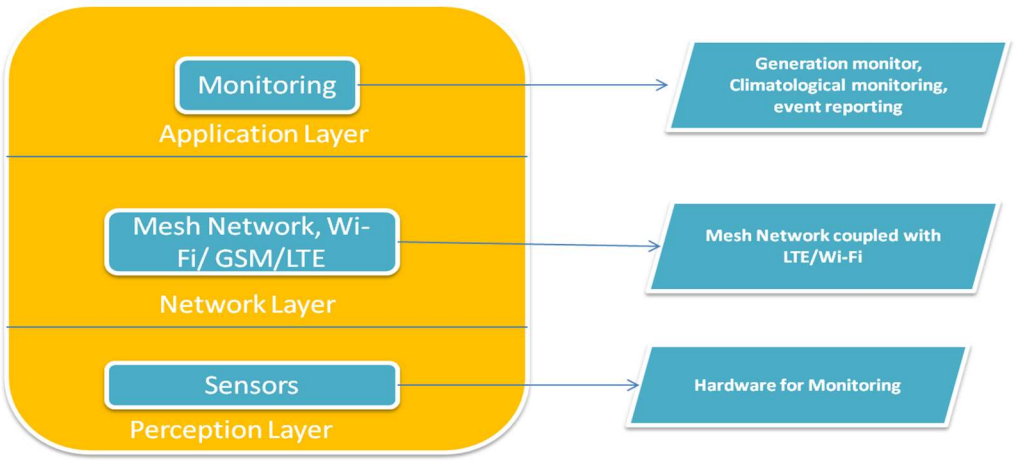

Figure 2.3 Structure of the communication network.

This figure states the flow of information and working of communication network in the grid. Data is collected from different elements using sensors. This data is relayed through the network to a local/cloud database. Monitoring and analysis are then implemented on this database.

2.2.1 Sensors

The devices that require integration with sensors are: inverter, *PV* converter, battery, individual meters, and weather station if any installed. With the advent of fourth industrial revolution, these elements are being released with at least one of the following

communication interfaces enabled: Bluetooth 4.0 (BLE or Bluetooth Smart), IEEE 802.11g (Wi-Fi), IEEE 802.3 (Ethernet), GPRS (2G telecom), HSPA (3G telecom) or Modbus Remote Terminal Unit communication. Microcontrollers available today come with most of these communications enabled with built-in two-way communication. Sometimes, additional hardware can also be used with a microcontroller to facilitate communication between the elements that need monitoring. Figure 2.4 illustrates the communication interface capabilities of a widely-used microcontroller raspberry pi, which can be used in the applications like this research work.

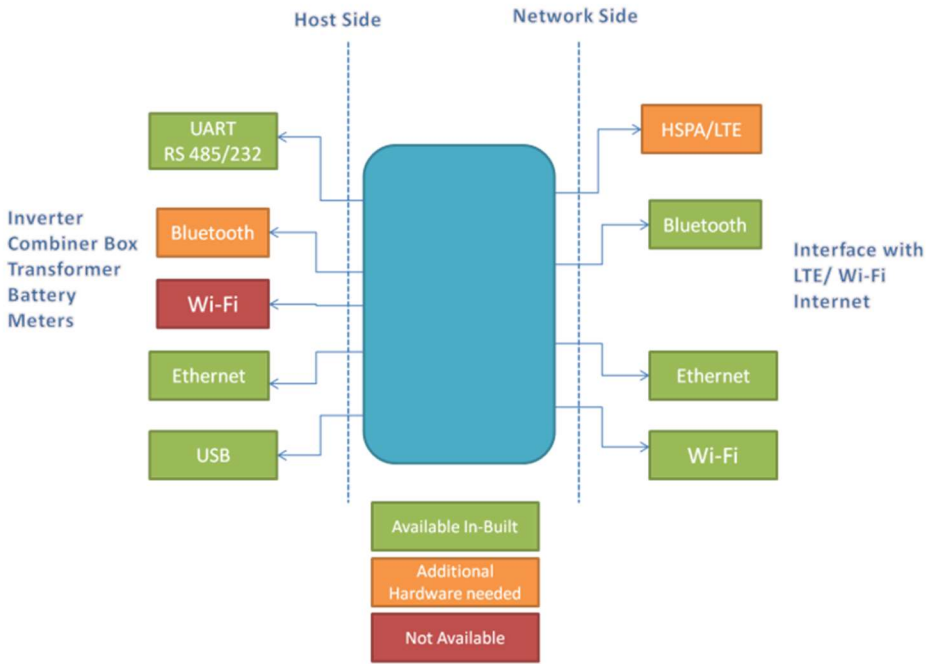

Figure 2.4 Communication capabilities of raspberry pi.

2.2.2 Network

Due to the virtue of being spread over a large area, smartgrid communication network is always a combination of different network configurations. In most cases, a Home Area Network (HAN) gets connected to Neighborhood Area Network (NAN) which in turn relays the data through a Wide Area Network (WAN) to internet or desired end user.

In this research work, we consider a network configuration based on mesh network topology. A mesh topology is a topology in which all the network nodes are individually connected to most of the other nodes. There are two configurations of this topology:

1. Fully connected, where all the nodes are connected to every other node.
2. Partially connected, where it is not necessary for all nodes to be connected to each other.

Generally, mesh networks are preferred in short-range and medium-range communication network arrangements. However, the greatest advantage of mesh topology is that every node, can act as an individual router, hence making it easily scalable and light. By the virtue of its topology, which consists of redundant links of established communication paths between each node, the chances of communication failure are very rare. The data will always have at least one suitable path for the flow of data. The range can also be extended by simply adding a node and the messages can hop through the mesh back to the gateway, making this a robust arrangement. Finally, self-optimization is the

greatest asset for mesh networks. If one route happens to be slow, a mesh network can potentially find a better route and optimize itself. The data flow link function in a mesh network can be expressed as:

$$F = \{f_i(l)\} \tag{11}$$

Where, $f_i(l)$ is the flow in channel i; $\forall i \in N = \{1,2,..P\}$ and N is the number of orthogonal channels. $\forall l \in E$; E is the number of data connection links at a particular node. A transmission function that determines the transfer of data from a node v at time t with link l is defined as:

$$v^t(l) = 1, \text{ when link l is active at node } v \text{ at time } t \tag{12}$$

$$v^t(l) = 0, \text{ in every other case} \tag{13}$$

In a mesh network, to facilitate data transfer between different nodes, the communication should follow constraints pertaining to the principles and resources existing at the node, channel and the network. To assess the present channel resources, the link channel constraint is expressed as:

$$\sum_{\forall i \in N} v_i^t(l) \leq \tau(l); \forall l \in E \tag{14}$$

Where, $\tau(l)$ is total number of channels available for communication through a link l. Additionally, to use the radio resources of a node at time t, the constraint can be defined as:

$$\sum_{\forall l \in E} \sum_{\forall i \in N} v_i^t(l) \leq \vartheta(l) \tag{15}$$

Where $\vartheta(l)$ is total number of radio points available for communication through a link l.

In addition, preventing interference is critical to obtain a data that is free from noise and corruption. For example, at node α and its neighborhood $C(\alpha)$, if the link l in $S(\alpha)$ is active on channel i and s is the other node at the endpoint of the link, l is only active when all other channels on the link are idle. This constraint can be expressed as:

$$\sum_{l \in S(\alpha) \cup S(\alpha`)} v_i^t(l) \leq 1 \tag{16}$$

$$\forall \alpha` \in E(\alpha) \tag{17}$$

The flow in a channel i at time t on link l is expressed as:

$$f_i(l) = \frac{c_i(l) \sum_{t \leq T} v_i^t(l)}{T} \tag{18}$$

When we sum (18) over T,

$$\sum_{\forall i \in N} \frac{\sum_{t \leq T} \mathrm{v_i^t(l)}}{\mathrm{T}} \leq \tau(l) \tag{19}$$

If the mean utilization of a channel is defined as $u_i(l)$ which can be expressed as:

$$u_i(l) = \frac{f_i(l)}{c_i(l)} \tag{20}$$

Hence, the utilization of the entire network can be defined from (19), (20) as:

$$\sum_{\forall i \in N} u_i(l) = \sum_{i \leq N} \frac{f_i(l)}{c_i(l)} \leq \tau(l) \tag{21}$$

The communication network in this research work for the grid system's architecture is divided into two peripherals of individual mesh networks. On the consumption side, a short range, mesh network can be created for facilitating the communication between the household smart meters. This network is intertwined with the sensor at the inverter which is in then terminated at the internet gateway. On the generation side, the *PV* converter and

sensors connected to the battery system are also connected in an internal mesh and through network boost equipment; they are terminated at the local database which is connected to the internet gateway. From the internet gateway, relevant data is sent to the cloud infrastructure developed for carrying out monitoring, control and optimization activities. Figure 2.5 illustrates the architecture of the network designed in this research work.

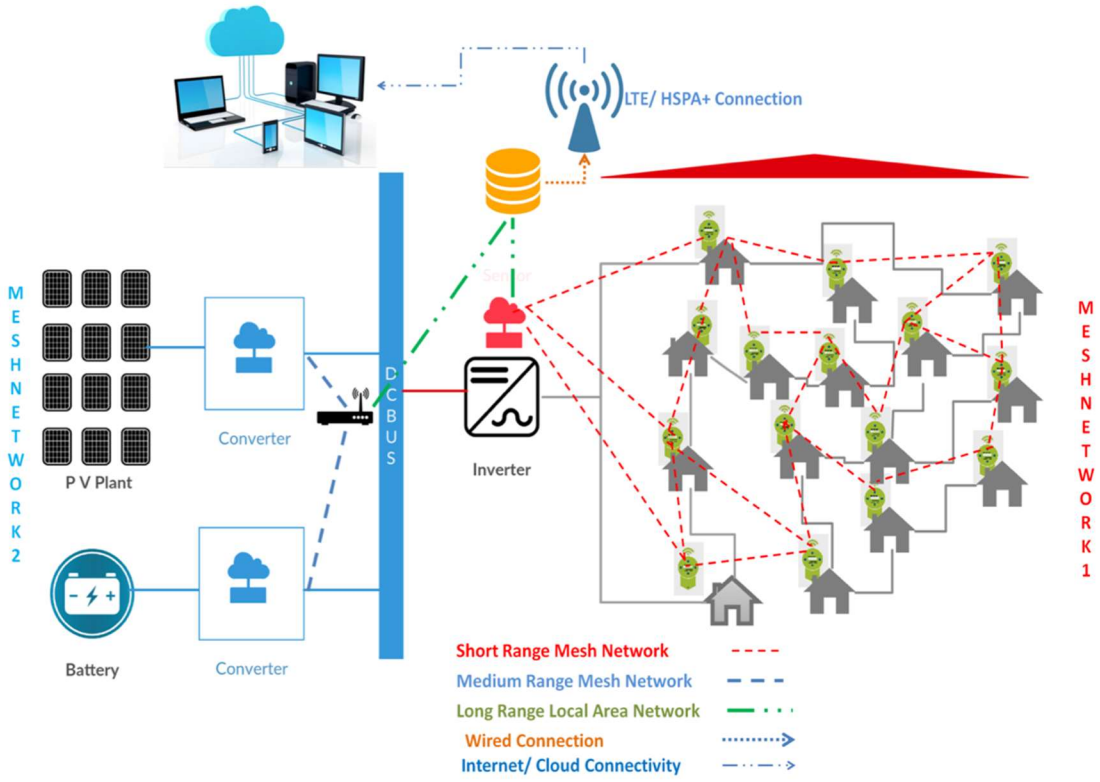

Figure 2.5 Communication Architecture of the Microgrid.

2.2.3 Data Flow

Each node in the network will periodically (as frequently as once in 5 seconds) publishes all measurements to the local database. All data would be stored in the local database, accessible to the operator via local monitors and to others via a cloud connection.

The cloud server is chosen in such a way to be capable of handling a high velocity of incoming requests from many devices that are concurrently connected, hence indicating a need for asynchronous and non-blocking operations. Upon login, the server shall send a response to the client (comet or long-poll architecture) to update all data and transfer more frequently.

The data will be represented block wise through an integrated monitoring platform that can be accessed through cloud. The data collected will include but not limited to the following parameters outlined in Table 2.1.

Table 2.1 Monitoring Parameters

Data Category	Parameters
General Data	• Timestamp • Device status • Temperature of device operating environment
Generation Data	• Inverter-specific data • Input DC voltage • Input DC current • Output AC line/phase voltage • Output AC line/phase current • Power factor • Frequency
Consumption Data	• Energy meter-specific Data of each household • Nearest transformer specific data
Climatological Data	• Ambient temperature • Global horizontal irradiance • Direct normal irradiance • Inclined irradiance • Wind speed

2.3 Monitoring and Performance Feedback

As per the data flow is outlined in the previous section, the data from each individual node in generation and consumption architecture gets tagged with their

respective data category in the database. The same database is replicated in the cloud software present in the remote server. Software is deployed on the cloud server to illustrate the data through a user interface and performance analysis on the data received. The functionalities of the software can be broadly classified into three parts:

1. Monitoring: The software reads the data with respect to the tag of the device, data category and interprets it on a user interface.
2. Feedback: The software verifies the data with respect to established rules and provides feedback about the status, working or problematic, if any at a particular element from the data it receives.
3. Control: Through the software, functions like shutdown, current flow or switching on/off of devices can be performed.

2.3.1 Monitoring

The inverter, *PV* DC output, battery status, energy meter status are the parameters that can be monitored and can be seen in the user interface as shown in Figure 2.6.

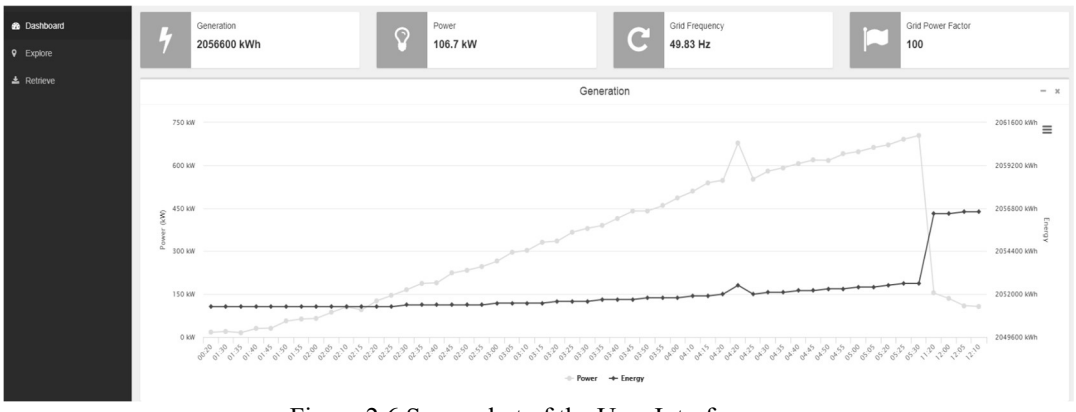

Figure 2.6 Screenshot of the User Interface.

Climatological data can also be represented in the interface from the weather station installed in the location or the data can be fetched using open source weather data providing solutions. The user interface can also be customized to better understand behavior of each element by creating profiles based on contextual data from connected devices. This can help in getting a complete picture of what is happening by combining everything already known about the power generation and consumption architecture with incoming data from each of the nodes.

2.3.2 Feedback

2.3.2.1 PV Performance

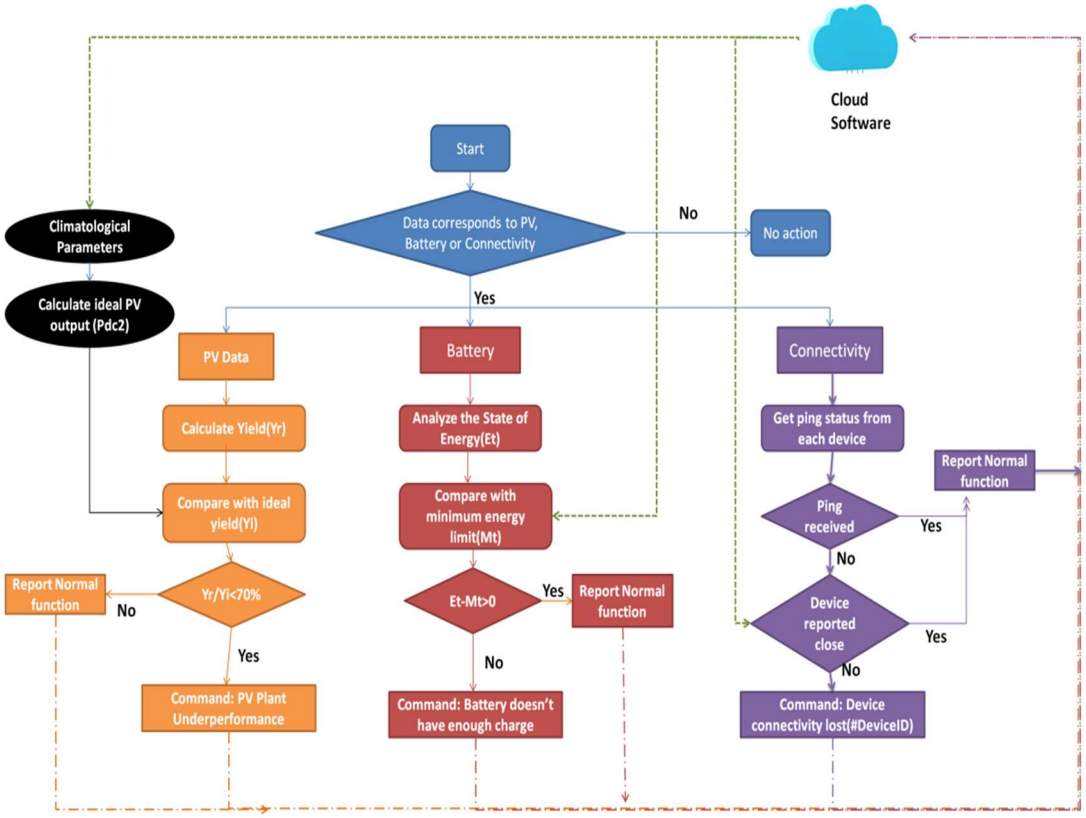

Figure 2.7 Decision chart of the proposed feedback mechanism.

Photovoltaic power generation, battery status and network strength are the three elements for which rules are established for performance monitoring. These parameters are continuously monitored for every 15 min and any related event is immediately reported. The rule base for each of the aforementioned three issues is illustrated in Figure 2.7.

For a *PV* plant, if the climatological parameters are available, a simulation model can be used, where the real-time weather parameters can be substituted in the model and

estimated power output at that given point of time can be calculated. However, there are tools like PVSyst [76] that can be used to obtain the data regarding ideal performance of a plant, at a given location with certain tilt angle and orientation. This can be compared with the real-time performance data to understand whether the plant is performing in an efficient manner.

The ideal performance of a *PV* system at a given location is the ration of total irradiance and reference irradiance. This can be expressed as:

$$Y_i = \frac{H}{G} \tag{22}$$

Where H is the total horizontal irradiance with units (Wh/m^2) and G is the global radiation at Standard Test Conditions (STC) measured in W/m^2.

It is to be noted that this value Y_i is highly dependent on the environmental variables like irradiance, temperature along with factors such as orientation and location (latitude). The actual yield Y_r, is calculated from the data obtained through monitoring the inverter and is expressed as:

$$Y_r = \frac{E_{PV}}{P_{max}} \tag{23}$$

Where, E_{PV}, is the energy output of the *PV* system in the interval considered and P_{max} is the peak power of the system at STC. Performance ratio can be expressed as:

$$P.R = \frac{Y_r}{Y_i} \tag{24}$$

This ratio can be defined as comparison of plant output to the ideal output of the plant at irradiation, panel temperature, availability of grid, size of the aperture area, nominal

power output, temperature subjected at the location of plant in the interval of measurement. Here, a threshold of 70-75% on the *P.R* can be installed to check for the performance and report for under performance in a given time interval.

2.3.2.2 Battery Status

Checking the battery status, to monitor the state of charge and energy present is important in this case, as the system is completely off-grid. Continuously monitoring the connectivity of the nodes is also important. If any connectivity issue is reported, immediate action can be taken to prevent further damage to the network. The following expressions elaborate on the battery threshold checking mechanism included in the feedback process.

$$E_{t+1} = E_t + (\eta_c * P_{t+1}^c - \eta_d * P_{t+1}^d - \varepsilon)\Delta t \quad (25)$$

$$\delta_{c,t+1} * P^{c,min} \leq P_{t+1}^c \leq \delta_{c,t+1} * P^{c,max} \quad (26)$$

$$\delta_{d,t+1} * P^{d,min} \leq P_{t+1}^d \leq \delta_{d,t+1} * P^{d,max} \quad (27)$$

$$\delta_{c,t+1} + \delta_{d,t+1} \leq 1 \quad (28)$$

Where,

E_{t+1} is the energy of battery at time t+1.

E_t is the energy of battery at time t.

P_t^c is the power charged by the *PV* system into the battery bank during the time t.

P_t^d is the power discharged by the battery bank to the load during the time t.

Δt is the time difference.

η_c is the charging efficiency.

η_d is the discharge efficiency.

$P^{c,min}$ and $P^{c,max}$ are the minimum and maximum power that can be charged into the battery respectively.

$P^{d,min}$ and $P^{d,max}$ are the minimum and maximum power discharge that can occur in the battery respectively.

ε : Self-discharge energy loss of battery.

$\delta_{c,t+1}$: Charge status of battery at time t+1.

$\delta_{d,t+1}$: Discharge status of battery at time t+1.

2.3.2.3 Mesh Network

The evaluation system is configured to alert the operator when there is no response to the ping between the devices and the database after three consecutive pings each at an interval of 5 secs. Time delay is a phenomenon that can be studied in two perspectives. One in the context of delay in data transfer and other in the context of delay in connection to a device due to network limitations. Delay in data transfer can be accommodated with a buffer time of 45 - 90 secs for the acknowledgement. For conditions of no network connectivity the feedback mechanism for network in Figure 2.7 alerts pertaining to the lost connectivity will be immediately notified to the operator.

2.4 Results and Discussion

To validate the proposed electrical and communication models, the electrical system was simulated with MATLAB Simulink in real-time. The Simulink design of the microgrid is illustrated in Figure 2.9. For a location in the country of Guinea in Africa, the temperature and irradiance profile are derived and illustrated in Figure 2.8 and 2.9. The parameters of the grid system as *PV* capacity and battery are calculated using the model described in [65] and the calculated values are expressed in Table 2.2. This table also consists of simulation parameters detailing peak power output and maximum battery status.

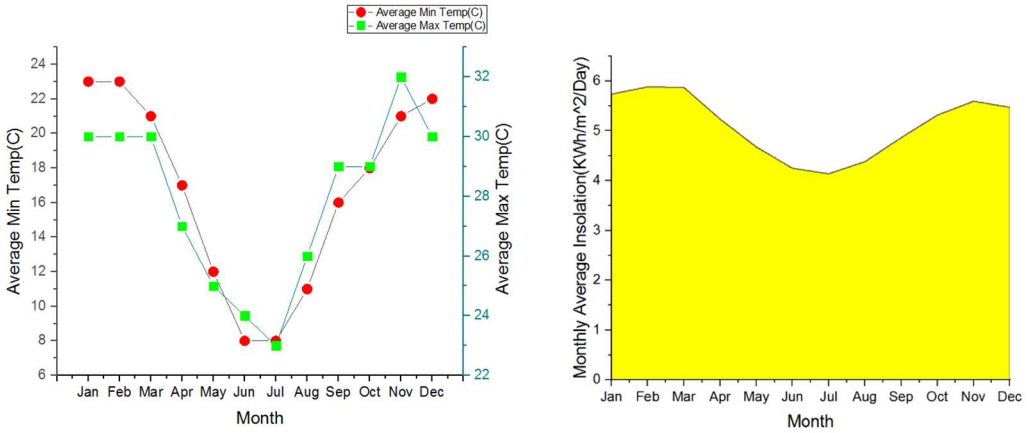

Figure 2.8 (a) Temperature profile of the location;(b) irradiance profile of the location.

Table 2.2 Parameters for Microgrid Simulation.

Element	Value
Number of households	75
PV system capacity	50 kW
Battery capacity	68 kWh
Average daily load requirement	98 kWh
Average Insolation	6.2 kWh/m^2/day

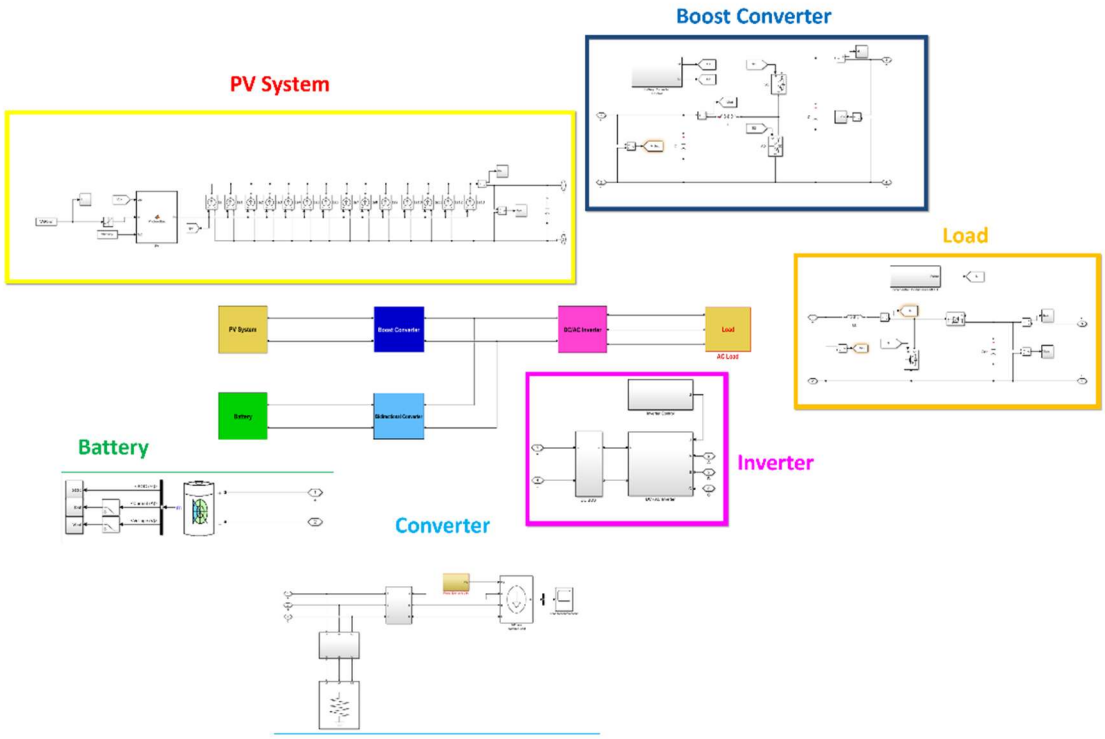

Figure 2.9 Simulink model of microgrid.

Figure 2.9 illustrates the simulated grid Simulink model of the system. The illustrated architecture contains mathematical models of a *PV* system, battery, *PV* converter, inverter and a bi-directional converter. The simulation runs for 3.04s. For *PV* system, a mathematical model that uses the irradiance, temperature inputs from the data of Figure 2.8 (a)-(b) is developed. For the load, the hourly load values as calculated in [67] and expressed in Figure 2.2 are used for the simulation.

Simulation results of the Simulink model for AC power, voltage, duty cycle and battery status is illustrated in Figure 2.10 (a,b). Maximum power of 47.25 kW is obtained at an irradiance of 950 W/m2 and 32 C.

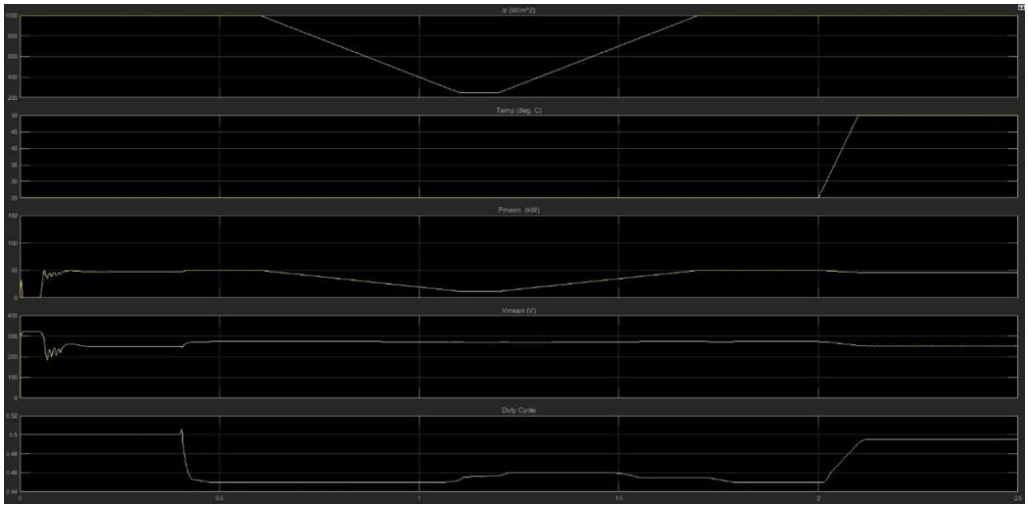

(a) AC power and Voltage Output of microgrid.

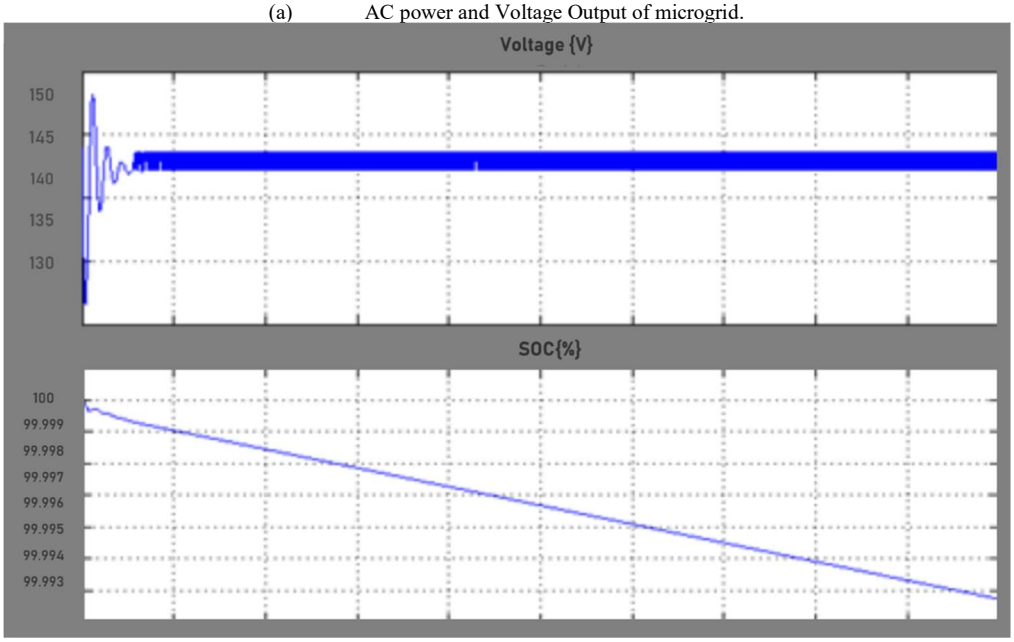

(b) Battery cycle and SOC of the storage in microgrid.

Figure 2.10 Simulation Analysis Results.

This Simulation was carried out with irradiance and temperature parameters for every month and the Yield values are recorded in a database. These yield values represent the reference or ideal yield values described in equation (11).

NSG2 software is used to build the architecture of the mesh network described in this research work. Figure 2.11 illustrates the simulation of a wireless mesh network for the grid system. Node N0 to N8 represent the consumption side while N12, N15 represent the PV converter and battery side of the network connection. N9 is the inverter node and N17 is the node of router that is used for boosting network availability. N9 is connected to N17 via wire where the data is cumulated in the local database.

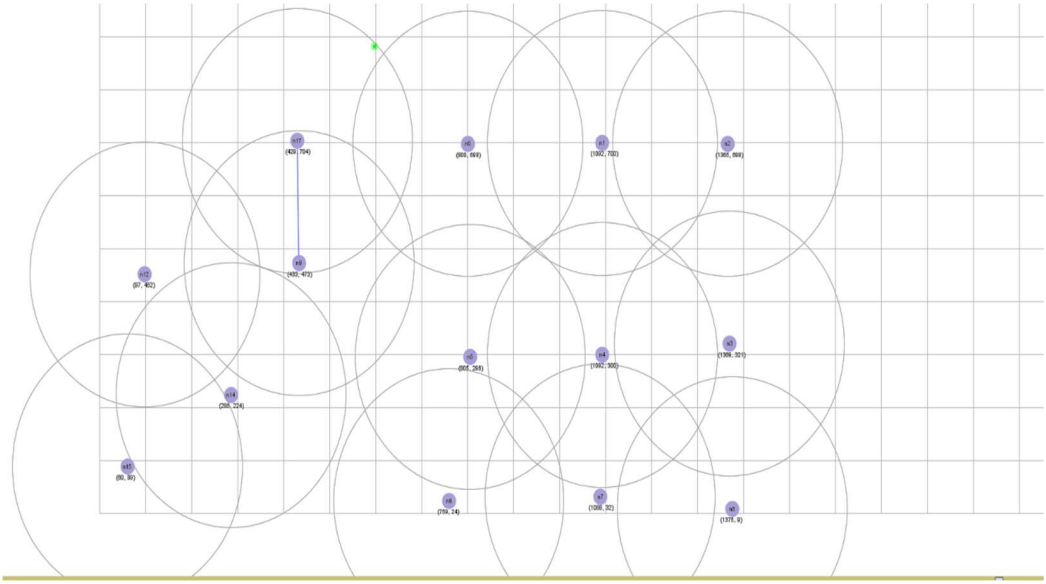

Figure 2.11 Microgrid Communication Wireless Model.

The grid simulink's model also consists of a feedback module interfaced with the output of PV generation and battery status as shown in Figure 2.12. This feedback module is programmed with the proposed mechanism illustrated in Figure 2.7.

Figure 2.12 The added Feed-back portion to the model.

This feedback module consists of an input data module for real-time data. This model can be used to feed the real-time performance data of a system and compare with the ideal performance as per (13) and the state of operation (underperformance or normal performance) can be communicated to the operator of the grid. To validate the working of the simulation with real-time data, performance of a rooftop 50kW system for a single day is collected along with the irradiance and temperature data from the sensors. These irradiance and temperature values are given as input to the system and the system is simulated without changing any of the other parameters. Figure 2.13 illustrates the comparison between the real-time value and ideal value.

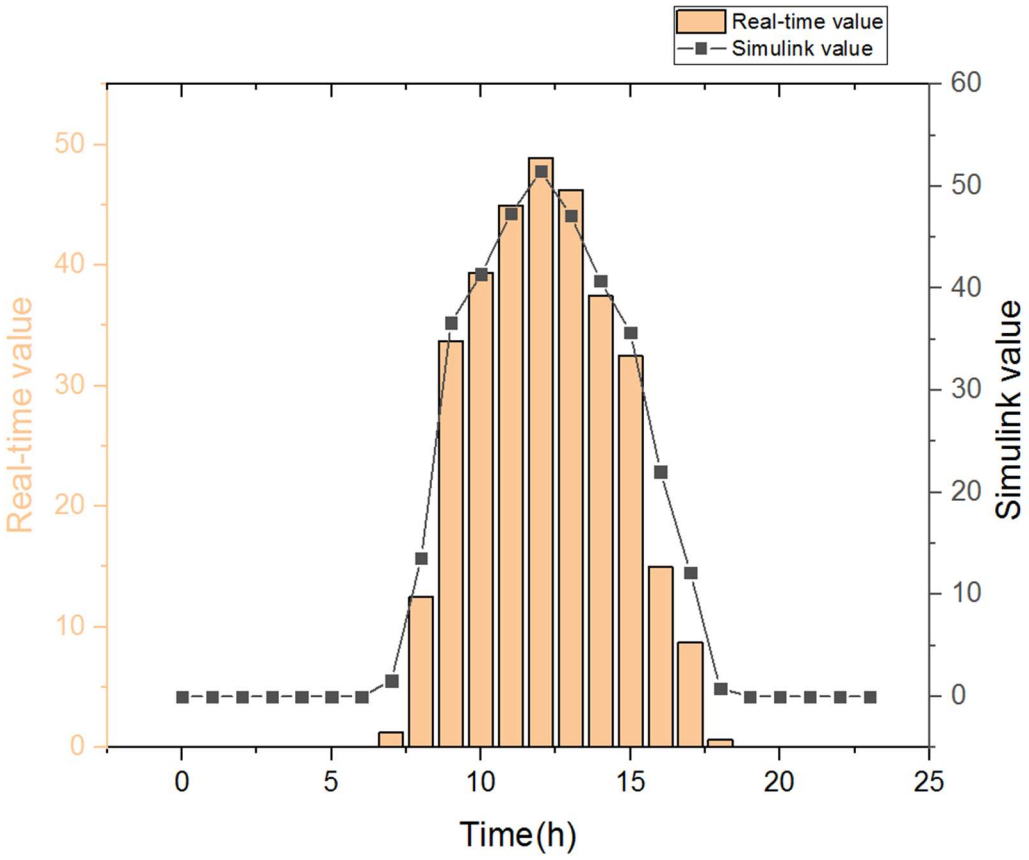

Figure 2.13 Comparison of Yi and Yr.

There are only two instances that are reported where the ratio of actual and ideal value is below 70% with an average ratio of 85.2%. The evaluation system is configured to alert the operator when there is no response to the ping between the devices and the database after three consecutive pings each at an interval of 5 secs.

In this research work, an integrated architecture intertwined with mesh networks is proposed for carrying out Feed Back oriented monitoring as well as computation of ideal performance and diagnosing the reasons for underperformance. This integrated architecture which is a combination of sensors, network elements, data base and

computation elements is designed specific for PV powered smart and microgrids. This architecture is designed on modular basis, which can be extended based on the number of nodes in the system. Apart from this, the network resilience and redundancy for smooth and loss less communication is another distinctive factor in this research work.

CHAPTER THREE: PV PERFORMANCE DIAGNOSIS THROUGH INVERTER DATA USING DEEP NEURAL NETWORK ARCHITECTURE

3.1 PV Characterization

Numerous solar cells are linked in series to make a PV panel of specific open circuit voltage (V_{oc}) and short circuit current (I_{sc}) and hence the effective power output, mentioned in terms of maximum power (P_{max}). Several PV panels are connected in series/parallel to shape an array to generate bulk power to meet the requirements of energy needs of a given population. Output current (I) and voltage (V) depend on the photocurrent (I_L) received by the cell.

The output current of a PV array with n_p umbers of panels connected in parallel can be expressed as in [68]:

$$I_{PV} = n_p I_P - n_p I_r \left[e^{\frac{q \quad V_{PV}}{kT_c A \ n_s}} - 1 \right] \tag{29}$$

Where,

q is charge; k is the Boltzmann's constant; A is the ideality factor of a p-n junction; I_P is the current of one PV panel; n_p is the number of panels in an array; I_r is the reverse saturation current expressed as function of temperature given by:

$$I_r = I_{rr}\left[\frac{T_C}{T_{ref}}\right]^3 e^{\frac{qE_g}{kA}\left[\frac{1}{T_{ref}}-\frac{1}{T_C}\right]} \quad (30)$$

Where,

T_c is the cell temperature; T_{ref} is the reference temperature and E_g is energy band gap of a solar cell.

At a given irradiance *S*, the output of current of a PV cell is expressed by the implication of temperature (*Tc*), irradiance(*S*) and voltage constant of cell (K_v) as:

$$I_P = 0.01\left[I_{sc} + K_v\left(T_c - T_{ref}\right)\right]S \quad (31)$$

Multiplying (29) with output voltage V_{pv} of a panel, the power output (P_{pv}) of an array is calculated as:

$$P_{PV} = n_p I_P V_{PV} - n_p I_r V_{PV}\left[e^{\frac{q\ V_{PV}}{kT_cA\ n_s}} - 1\right] \quad (32)$$

Substituting (31) in (32), the output of power can be expressed as:

$$P_{PV} = n_p 0.01\left[I_{sc} + K_v\left(T_c - T_{ref}\right)\right]SV_{PV} - n_p I_r V_{PV}\left[e^{\frac{q\ V_{PV}}{kT_cA\ n_s}} - 1\right] \quad (33)$$

Predominant factors prompting the output of power of a given PV array are irradiance received by a panel and its surrounding temperature. In addition, findings reported in [69] show the effect of wind speed and humidity on efficiency of a PV panel output. Hence, these two additional factors were also considered for better training of ANN in this research work. A PV system with poly crystalline solar cell, Sun power make 315W

solar module is used with V_{oc}=64.6 V and I_{sc} = 6.14 A. Twelve such panels are linked in series to construct a single array and twenty-five of them are connected together to provide power to 100kW inverter connected at each node. DC power output is calculated using (33) with real time data available from weather monitoring station. Since most of the large scale/utility power plants are connected to AC grid, inverter efficiency (conversion of DC power accessible from PV array to power fed to AC grid) plays an important role in performance evaluation of overall plant. Inverter power output is directly related to its operating point and conversion efficiency along with in-built maximum power point tracking (MPPT). Generally, inverter manufacturers provide the data sheet pertaining to the efficiency vs. percentage of rated power output or irradiance.

3.2 Performance Evaluation

Regular performance analysis of solar plants can help in addressing the issues related to reliability in early stage of their installations before they affect the power generation significantly. It also helps in getting an indication in the strategy, framework, operation and maintenance of upcoming connected smartgrid systems. Performance evaluation of a PV system is generally identified with two aspects, efficiency of elements in the system and efficiency of performance of the system with respect to climatological parameters. Overall efficiency is product of individual efficiency of PV arrays, inverters and overall effectiveness. Efficiency of PV system (η_{PV}) is the global efficiency factor of

a solar panel, where it is defined as the percentage of incident light energy that is converted into electrical energy by a solar panel.

Efficiency of inverter (η_{Inv}) is expressed as the ratio of the AC power output (P_{AC}) and DC power input (P_{DC}): $\eta_{Inv} = \frac{P_{AC}}{P_{DC}}$

and its typical range is 93-95% and PV plant efficiency is given by:

$\eta_{Plant} = \eta_{PV} * \eta_{Inv}$

Other performance parameter includes performance ratio (PR) defined in terms of actual energy yield of a plant (Y_R) and the ideal energy yield (Y_I) for a given duration:

$PR = Y_R/Y_I$

and capacity utilization factor (CUF) given by:

$$C.U.F = \frac{E_{PV}}{365 * 24 * P_{ins}}$$

Where, E_{PV} is energy in kWh of the PV plant for a year and P_{ins} is the installed capacity of the PV plant in kW.

Energy yield using parameters like solar irradiance, temperature, tilt angle, latitude of the location is generally calculated using automated computer aided tools like, Pvsyst [66]. However, these tools can only give a generalized estimate of energy available at a given location and often fail to address local factors responsible for power loss like soiling, partial shading, hot spot and other physical wear and tear over a period. Therefore, an artificial neural network model is developed from existing performance data of a solar power plant to accurately predict electrical energy available over entire duration of its

operation. ANN output is exploited as a reference to relate real-time output of the solar power system to continuously evaluate and monitor the performance efficiency.

3.3 Mesh Network Architecture

As mentioned in chapter 2 mesh networks are used in this research work due to their redundancy in node communication where there is always a path for communication if there is a failure of communication at a particular node. In this chapter a mathematical optimization is used to find the optimum path for the mesh network proposed in chapter 2 and route the data in the mesh network. For a given mesh network where:

N: total nodes

D: total wavelengths per fiber

U_{ab}: total of fibers between a and b

T: total transmitters at a node

R: total of receivers at a node

C: channel capacity or wavelength

Λ: information matrix of traffic set.$\Lambda = \Lambda_n$, in which n can be any permissible less pace flow, 1, 3, 12, etc. In this research work i $\in \{3,5,10\}$

Variables:

- V_{mn} is number of node to node virtual paths in virtual topology and V^{λ}_{mn} number of virtual paths between nodes conducted via fiber link on wavelength λ.
- B^{λ}_{mn} number of physical paths among nodes conducted via fiber on wavelength λ.

- $\Upsilon^{sd,t}_{mn,i}$: The t^{th} OC-i demand of less pace traffic where node s to node d occupying path (m,n) as an intermediary virtual link.
- $P^{i,t}_{sa}$ $P^{i,t}_{sa}$ =1, only when the t^{th} OC-i demand of less pace link where node s to node d accurately dispatched; otherwise, $P^{i,t}_{sa}$=0.

Hence for facilitating the optimal data flow the optimization function is given by amplify the total successfully dispatched low-speed traffic (f) where:

$$\text{Max f} = \sum_{i,s,d,t} i * P_{sd}^{i,t} \tag{34}$$

With constraints, as:

$$\sum_n V_{mn} \leq T_n \qquad \forall m \tag{35}$$

To verify that the total quantity of paths between node pair (m,n), is fewer than or equal to the total number of communicators (transmitters) at node m.

$$\sum_m V_{mn} \leq R_n \qquad \forall n \tag{36}$$

To verify that the total quantity amongst node pair (m,n) is fewer than or equal to the number of recipients at node n.

$$\sum_\lambda V_{mn}^{\lambda} = V_{mn} \qquad \forall m, n \tag{37}$$

Here is to verify that the paths between m, n contain paths which have different wavelengths among the pair (m,n).

$$\sum_i B_{ik}^{mn,\lambda} = \sum_j B_{jk}^{mn,\lambda} \qquad \text{if } k \neq m, n \ \ \forall m, n, k, \lambda \tag{38}$$

To verify intermediary node k of route (m,n) existing in wavelength λ and total number of inward and outward route flow are equal.

$$\sum_i B_{im}^{mn,\lambda} = 0 \qquad \forall m, n, \lambda \tag{39}$$

To verify source node (m) of route (m,n) existing in wavelength λ and total number of inward route flow are equal 0.

$$\sum_j B_{nj}^{mn,\lambda} = 0 \qquad \forall m, n, \lambda \tag{40}$$

To verify end node (n) of route (m,n) existent in wavelength λ and total number of outward route flow is 0.

$$\sum_j B_{mi}^{mn,\lambda} = \sum_j V_{mn}^{\lambda} \quad \forall m, n, \lambda \tag{41}$$

To verify source node (m) of route (m,n) existent in wavelength λ and total number of inward route flow is equal to the overall quantity of routes amongst node pair (m,n) existent in wavelength λ.

$$\sum_i B_{in}^{mn,\lambda} = \sum_j V_{mn}^{\lambda} \quad \forall m, n, \lambda \tag{42}$$

To verify end node (n) of path (m,n) existent in wavelength λ and the sum of outward route flow is equal to the overall quantity of routes among node pair (m,n) existent in wavelength λ.

$$\sum_{mn} B_{ij}^{mn,\lambda} \leq \sum_j B_{ij}^{\lambda} \quad \forall i, j, \lambda \tag{43}$$

$$B_{ij}^{mn,\lambda} \in \{0,1\} \tag{44}$$

(43-44) are to guarantee the wavelength λ on a single path (m, n) is existent in a max of only a single path in the network.

$$\sum_m \Upsilon_{md,i}^{sd,t} = S_{sd}^{it} \tag{45}$$

$$\sum_n \Upsilon_{sn,i}^{sd,t} = S_{sd}^{it} \tag{46}$$

For (45), (46):

$$\forall s, d, t \quad \text{i} \in \{3,5,10\} \quad t \in \left[1, \Lambda_{\text{i,sd}}\right] \tag{47}$$

$$\sum_m \Upsilon_{mk,i}^{sd,t} = \sum_n \Upsilon_{kn,b}^{sd,t} \text{ if } k \neq s, d \;\; \forall s, d, k, t \tag{48}$$

$$\sum_m \Upsilon_{ms,i}^{sd,t} = 0 \tag{49}$$

$$\forall s, d, t \quad \text{i} \in \{3,5,10\} \quad t \in \left[1, \Lambda_{\text{i,sd}}\right]$$

$$\sum_n \Upsilon_{dn,i}^{sd,t} = 0 \tag{50}$$

$$\forall s, d, t \quad \text{i} \in \{3,5,10\} \quad t \in \left[1, \Lambda_{\text{i,sd}}\right]$$

$$\sum_{i\,t} \sum_{s\,d} \text{i} * \Upsilon_{mn,i}^{sd,t} \leq V_{mn} * C \;\; \forall m, n \tag{51}$$

$$S_{s\,d}^{i\,t} \in \{0,1\} \tag{52}$$

Eq. (48) – (52) to guarantee routing of less pace flow requirements on fundamental architecture, furthermore considering and cogitating that all channels, along with their wavelengths capabilities, ought to be closely monitored for the entire passing flow (data flow) not to exceed their capacities.

In this research work [36], 8 PV generation systems are distributed over an area of 5 acres is chosen where each PV system capacity is 25kW conquering the aggregate generation capacity up to 200 kW. The minimum distance between every system is illustrated in Fig 3.1.

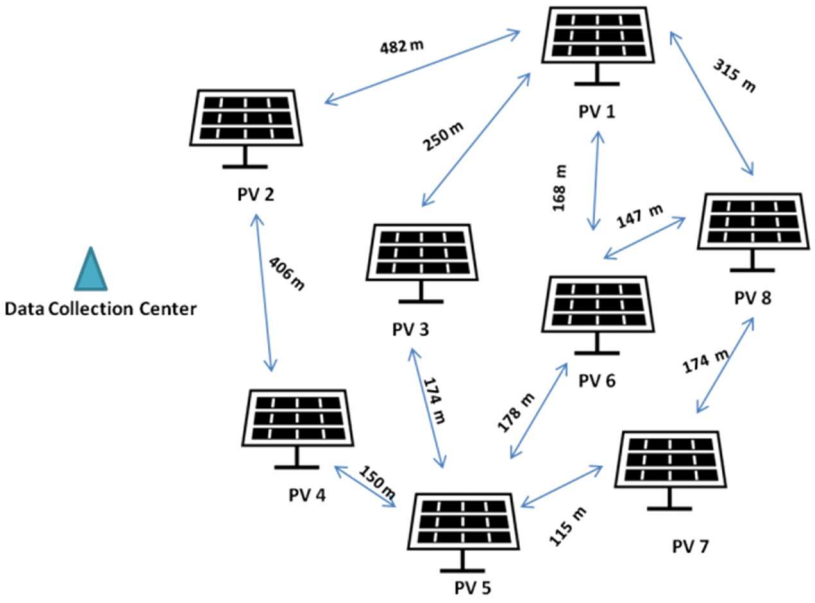

Figure 3.1 Minimum distance between PV systems.

Mesh networks algorithm discussed above is used to find an optimum path for data transfer from these systems to a centralized data collection center illustrated in Fig 3.1. The distance parameters and network constraints are given as input in NS2 open source software and two optimum path l1& l2 are obtained using the constraints (35-44). These are illustrated in Fig 3.2 and 3.3 where the arrows signify the transfer of data from one node to another. It can be seen that in both configurations redundant path exists to make sure that there is no interruption in data transfer if one node malfunctions.

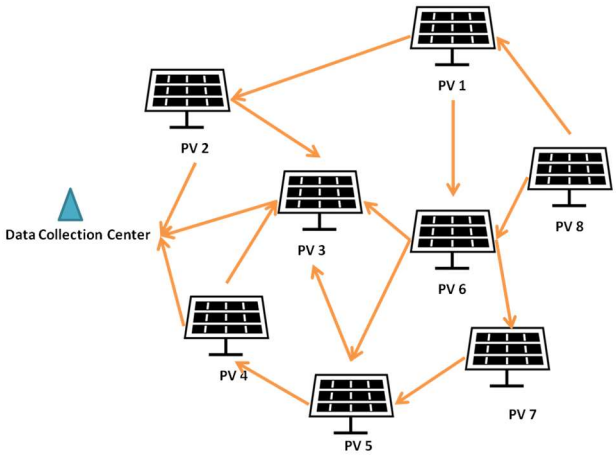

Figure 3.2 Configuration l1

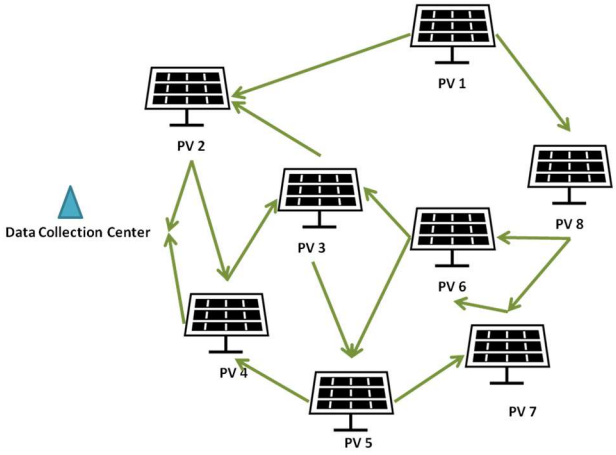

Figure 3.3 Configuration l2

The operational parameters for l1 and l2 as a result of the simulation are expressed in Table 3.1.

Table 3.1 Mesh Network Operational Parameters

Parameter	L1	L2
Throughput (Kbps)	50011	51274
Latency (sec)	0.00208	0.00320
Packet Delivery Ratio (%)	99	99
Network Life Time(min)	507.174	499.361
Routing overhead (%)	99.46	99.17

3.4 Artificial Neural Networks

In the last couple of years, artificial neural networks have gained tremendous reputation since they have numerous progressive abilities for statistically classifying and identifying. Utilizing ANNs is achieved by formulating nonlinear data to be categorized and identified by pattern based on designated mathematical functions. The anatomy of rudimentary artificial neural network can be defined as input, output and hidden layers; hence both ends have depots, such as architecture is demonstrated in Fig. 3.4.

An artificial neural network with multilayer perceptron is presented and it is constituted and designed by means of Levenberg Marquardt algorithm [30] as follows:

- Encoded number of input parameters along with hidden layers quantity besides every hidden layer neurons. Also for every layer, predefining and configuring weights and biases.
- Predefined weight ($w_{i,l}$) is multiplied with the input arguments (I_i) in input layer considering summing it with the bias of the node ($b_{i,l}$) as:

$$a_{1,1} = \left(\sum_{i=1}^{n} I_i w_{i,1}\right) + b_{i,1} \tag{53}$$

- The frequently used activation function which is (tan or log) sigmoid, where summation (53) is computed, as:

$$\sigma(a_{1,1}) = \frac{1}{(1+e^{-a_{1,1}})} \tag{54}$$

- Activation function yield will be used to feed next layer in which it is the input and this process happens repeatedly in all following layers until grasping end node.
- Once the end node is attained, then the results are compared with the designated rule for this training process..
- Mean Square Errors (MSE) and Mean Square Deviation (MSD) are two of the effective widely used methods of systems measurements:

$$MSE = \left(\frac{1}{n}\sum_{i=1}^{n}\sum_{j=1}^{k}\left(t_{i,k} - o_{i,k}\right)^2\right) \quad (55)$$

  In which, $t_{i,k}$ is desired limit and $o_{i,k}$ is outcome.
- Utilizing those measurements will assist in revising biases and weights in the desired structure of such a network for better results in the next round of trainings and testing.
- Input, training, testing and output is done repetitively until a threshold or a targeted value has been achieved.
- Generally, ANNs can work cleverly by taking into account updating trajectories for improved outcome and accomplishing desired fallouts.

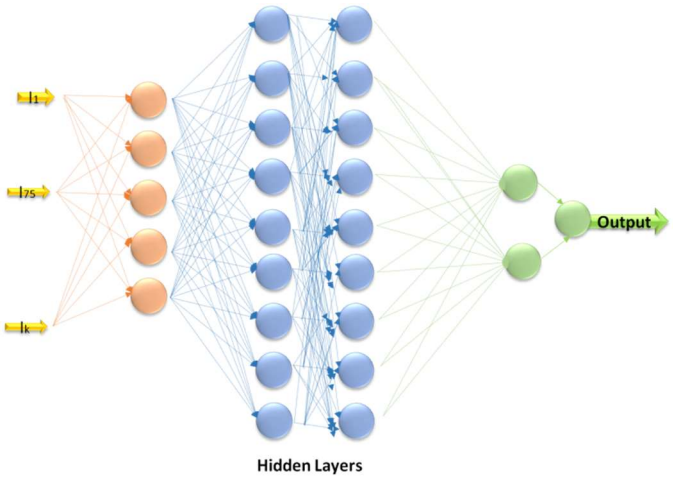

Figure 3.4 Neural network model.

The propositioned model's accurateness is around 99.7%, although the MSE of the neural network model's is approximately 0.00548 as shown in Fig. 3.5

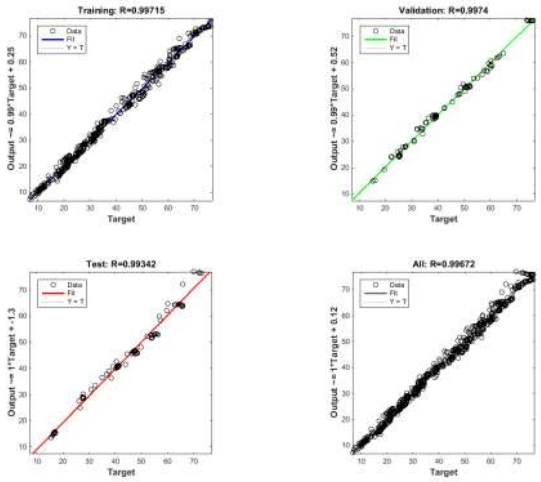

Figure 3.5 Training, Testing and Validation Result.

Figure 3.6 displays the comparison of the error value for the 3rd of March for the whole day. A maximum error of -0.68 is obtained at 14:24 hrs on the day while calculating the power output and a minimum error of -0.42 is obtained at 13:00 hrs.

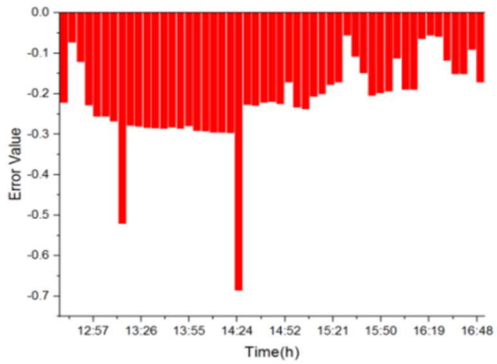

Figure 3.6 Comparison of actual and estimated power output.

Fig. 3.7 illustrates the average percentage error for the whole year while on predicting the productivity of the PV system. The highest percentage error of 6.82% is reported during 12:30-1:30 pm in the month of February as well as in June. In the negative trend side, around -4.8% error is obtained during 12:45-1pm in the month of January and -5.2% during the same time in February and September.

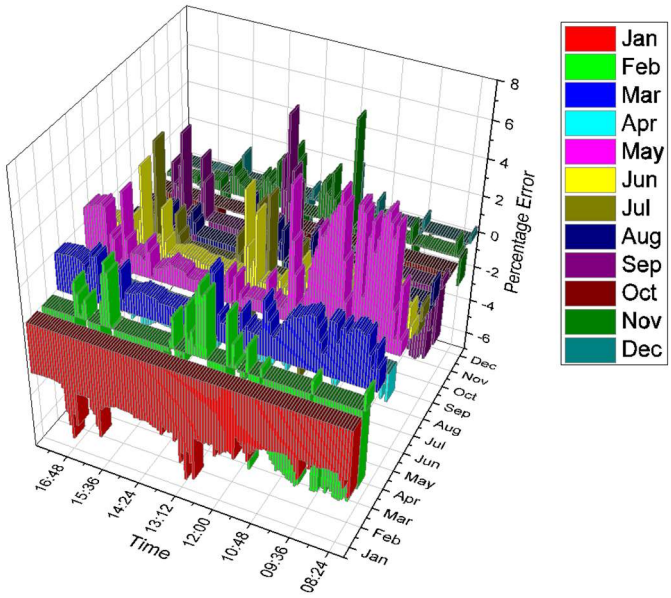

Figure 3.7 Percentage error for power prediction during entire year.

3.5 Dynamic Performance Prediction (Without Deep Neural Network)

Real time performance prediction and evaluation is critical to understand the efficiency of the system and can help as an indicator regarding the health of different elements of the system. After network initialization, the real-time performance data of the solar plants along with the weather station data is logged in the central database at an interval of 5 minutes as shown in Table 3.2. This database is based on Denver, Colorado data and is interfaced with the neural network model in the same workstation. After every half an hour, the neural network model fetches date and time from the system and sends a request to the database for obtaining the climatological parameters that serve as input to the system. An independent program in the workstation, then randomly picks the value of a single instance out of six instances that occurred in the past half-an-hour in the database and feeds them subsequently to the MATLAB program.

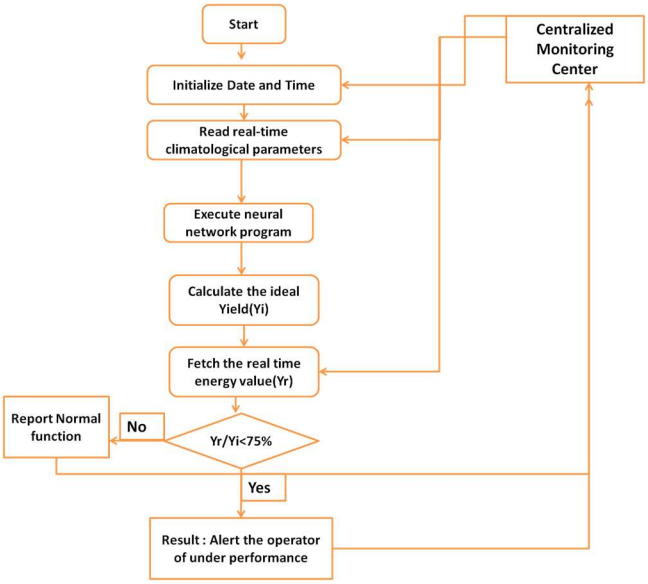

Figure 3.8 Flow chart for dynamic performance evaluation.

Table 3.2 Real-time input from the network database

Date	Time	Irradiance DNI(W/m2)	Ambient Temperature©	Humidity (%)	Wind speed(m/s)	Voltage PV(V)	current(I)	Array DC power(kW)	Inverter efficiency(%)
1-Mar-18	12:30:02	633	19	40.2	2.8	394.973	37.1685	3.477	97.1886
1-Mar-18	12:35:02	633	19	40.2	2.9	394.981	37.215	3.479	97.1801
1-Mar-18	12:40:02	639	19	40.2	3	394.980	37.50829	3.482	97.1750
1-Mar-18	12:45:02	639	19	40.2	3	394.982	37.4987	3.501	97.1702
1-Mar-18	12:50:02	638	19	40.2	3	394.987	37.45164	3.522	97.1642
1-Mar-18	12:55:02	637	18	40.2	3	394.991	37.39499	3.602	97.1575
1-Mar-18	13:00:03	638	18	40.2	3	394.995	37.45162	3.687	97.1498
1-Mar-18	13:05:02	638	18	40.2	3	394.998	37.45162	3.784	97.1449

The neural network model executes with the input provided, calculates the output and sends it to the independent logical program in the workstation. The real-time performance value of power output corresponding to the input parameters is fetched by the program and then compared to the estimated output. If the ratio of real time value and estimated value is less than 75%, which is the average performance ratio of a plant at the installed location, an alert is generated in the workstation regarding the underperformance of the system, which is presented in the flow chart in Fig. 3.8.

Underperformance of a PV system can be characterized as hinderance in performance due to shading, soiling, equipment damage. In this research work, soiling and shading are considered, and performance data is used to model this system.

Interactive user interface with real time energy production data is shown in Fig. 3.9. The average mean time for response is noted as 5.36 sec with the quickest response time of 2.18 sec in case of normal performance and slowest response time of 7.92 sec in case of underperformance. The number of instances collected in a full year and the statistics related to the performance evaluation are given in Table.3.3.

Table 3.3 Statistics for dynamic performance evaluation

Parameter	VALUE
Number of instances collected	43240
Number of instances selected for performance evaluation	15060
Number of times PR reported <75%	4201
Percentage of instances where underperformance is reported	27.8%
Average mean time for response (sec)	5.36(Min 2.18, Max 7.92)

Figure 3.9 User interface for notifying operator.

Application of the proposed communication infrastructure while integrating neural network-based computation or performance diagnosis as well as rule-base based mechanism is a significant contribution in this research work. Voluminous state of art communication infrastructures in the prevailing literature propose a single aspect/task-oriented application like monitoring, data storage etc. However, in this research work a multi-faceted application of the infrastructure was elaborated as follows:

- Features of PV generation, battery status are monitored and are integrated through network along with feedback based measures for effective performance in the smartgrid.

- Real-time performance data was collected at a centralized database while ideal performance was calculated and compared for diagnosing critical performance issues of solar power generation like soiling and partial shading.

3.6 Underperformance Diagnosis with Deep Neural Networks

Deep Neural Networks (DNN) as shown in fig. 3.10 are different from single-hidden-layer neural networks due to their depth or number of node layers through which the data is subjected [71]. These layers establish a multistep process of feature extraction and pattern recognition that increases the efficiency of the DNN.

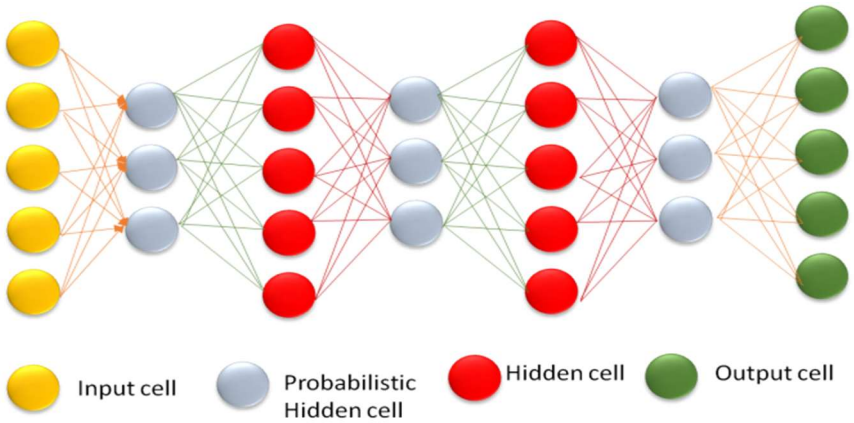

Figure 3.10 Deep Neural Network Architecture.

A solar panel output is dependent primarily on irradiance and temperature of the location. The system output is a function of number of panels, their connection architecture and the inverter characteristics. In every juncture of this performance characterization the non-linear dependence of variables on the power output can be clearly observed. To address this high nonlinearity, a Deep Belief Network (DBN) class of DNNs is used to model the performance.

A DBN is a class of DNN with multiple hidden layers connected through layers instead of individual neurons in the layers [23]. A DBN can learn to probabilistically reconstruct its inputs and extract features. Restricted Boltzmann Machines (RBM) networks are used in this research work for training due to its effective, fast and generative training procedure.

A Typical RBM has binary nodes in each layer denoted as a combination of visible layer (u) and hidden layer (k) as:

$$u = \{u_i\} \tag{56}$$

$$k = \{k_j\} \tag{57}$$

For any $\{u_i, k_j\}$ no intra-layer connection exists. A bidirectional connection, however exists and the probability to have a specific connection is determined by the energy vector E(u,k), expressed as:

$$p(u,k) = \frac{1}{Z} e^{-E(u,k)} \tag{58}$$

Where,

$$Z = \sum_{u,k} e^{-E(u,k)} \tag{59}$$

is the normalization factor.

The energy vector E in the form of the bias vector of hidden layer b_k , the bias vector of visible layer b_u and weight matrix W between u and k can be expressed as:

$$E(u,k) = -b_u^T u - b_k^T k - u^T W k \tag{60}$$

The conditional distribution for connection between visible layer with hidden layer and vice versa can be expressed as:

$$p(u|k) = \prod_i^U p(u_i|k) \tag{61}$$

$$p(k|u) = \prod_j^K p(k_j|u) \tag{62}$$

Where U and K are total number of nodes in visible and hidden layers.

With a sigmoid activation function that can defined in (54), the probability of a node getting activated can be expressed as:

$$p(k_j = 1|u) = \sigma(b_{k,j} + u^T W_j) \tag{63}$$

$$p(u_i = 1|k) = \sigma(b_{u,i} + k^T W^T{}_i) \tag{64}$$

The weights are updated through a contrast divergence algorithm here k-step Gibbs sampling is performed to reconstruct the training data by:

$$\Delta w_{i,j} = \varepsilon(\langle u, k\rangle_{data} - \langle u, k\rangle_{recon}) \tag{65}$$

RBM acts as an effective data pre-processing or pre-training method to classify or cluster the input variables according to their common characteristics.

Input vector to ANN model is I = *[S_I T_I t_I d_I]*, where, *S* is irradiance; *T* is temperature; *t* and *d* correspond to the date and time at which PV power output is obtained.

The output vector is $O = [I_{C_1} V_{C_1}]$, where, I_{C_1} and V_{C_1} correspond to DC current and voltage output respectively. AC power is obtained from inverter characteristics.

The data obtained is subjected to RBM training and the output is illustrated in Fig.3.11. Through RBM, the features of the data points in context of irradiance and power

are extracted and the entire data set is clustered into 7 clusters. Every cluster corresponds to an irradiance and power level. For example, cluster 1 consists of data points pertaining to power output value in the range of 60kW . Similar is the case with cluster 4 where the data points corresponding to the power value of the range 20-30kW

It can be observed that at any irradiance value, there are two or more corresponding power output values. This arises because during the experimentation, artificial soiling and artificial shading experiments were conducted. While collecting the data, to create an exhaustive set of practical conditions on a solar panel, artificial soiling and artificial shading experiments are conducted on the panel and the data collected.

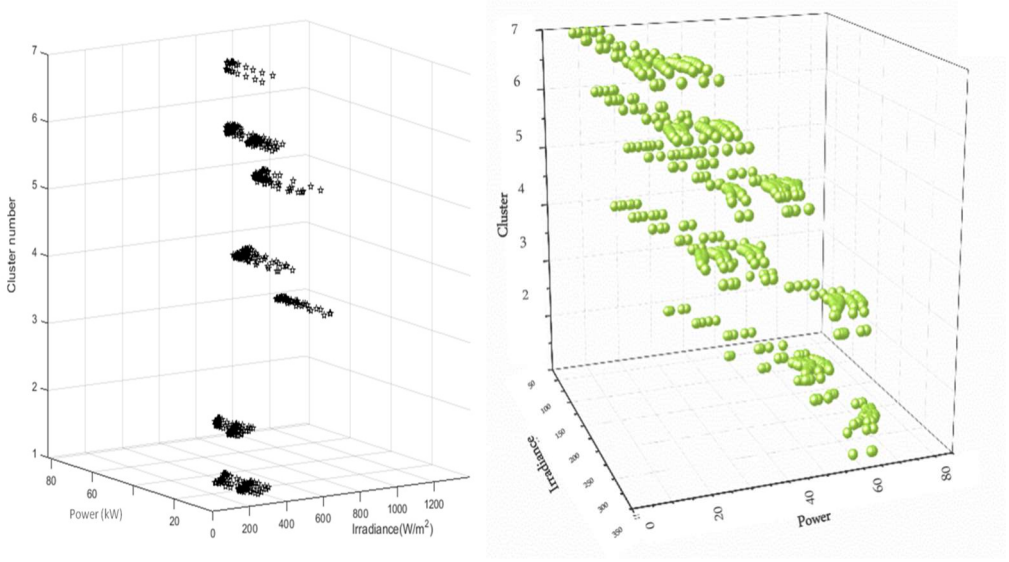

Figure 3.11 RBM output of the performance data.

Each of the anomalies is given a state value. In normal condition for ideal performance, the state condition value, s= 0. If the power output is obtained as a result of soiling the panel, s = 1 and for partial shading the value of s = 2.

After RBM classification, at each irradiance level the different power output values are assigned the state value (s). The irradiance, power output is used as inputs and the state value is used as output for a MLP neural network model. The model is simulated and a training efficiency of around 99.95%, validation efficiency of 99.3%, testing efficiency of 99.51% is obtained as shown in fig. 3.12.

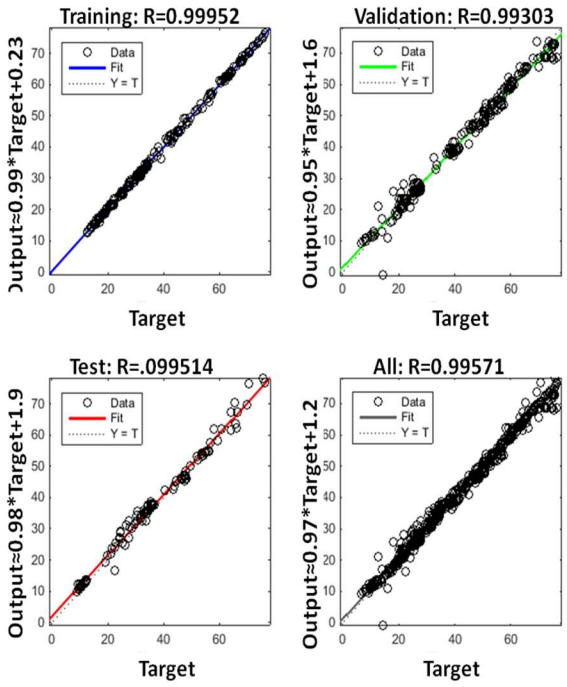

Figure 3.12 ANN simulation output.

The obtained model is now tested with real-time climatological data and the output obtained through the model is compared with the actual power output. Fig. 3.13 shows the comparison of the actual values and estimated value. The mean square error value in this comparison is 0.014.

Table 3.4 Statistics of Performance Diagnosis

Parameter		Value
Number of instances		21400
For s=0	Actual	14201
	Identified	14314
	False Positive	140
For s=1	Actual	5192
	Identified	4936
	False Positive	284
For s=2	Actual	2540
	Identified	2150
	False Positive	82

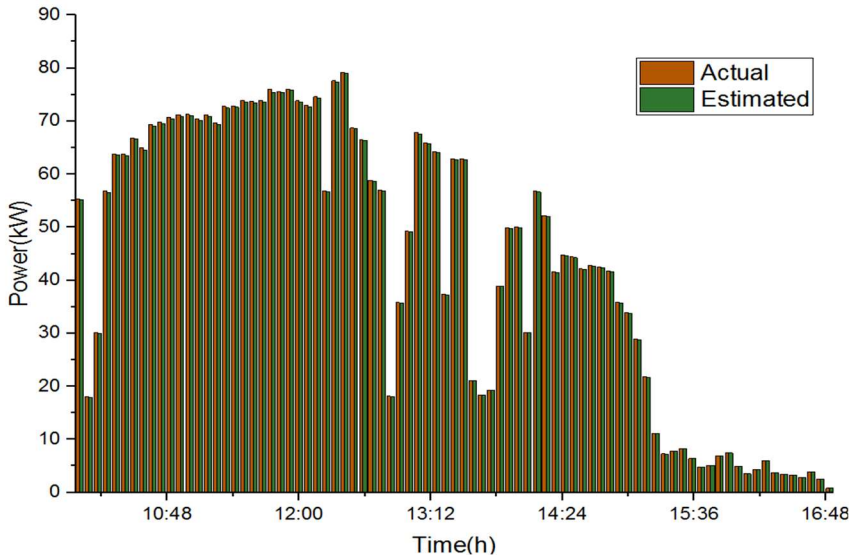

Figure 3.13 Comparison of actual vs estimated power output.

Actual power values are fed to the neural network in the second iteration to identify the state of performance of the system. This experiment is repeated for a period of 6 months and the results obtained for all the three states of s is expressed in Table.3.4. For s=0, the error of prediction is -0.8% while the value is 4.9% and 3.2% for s=1 and s=2.

Overview of the procedure followed in this research work is illustrated in Fig.3.14

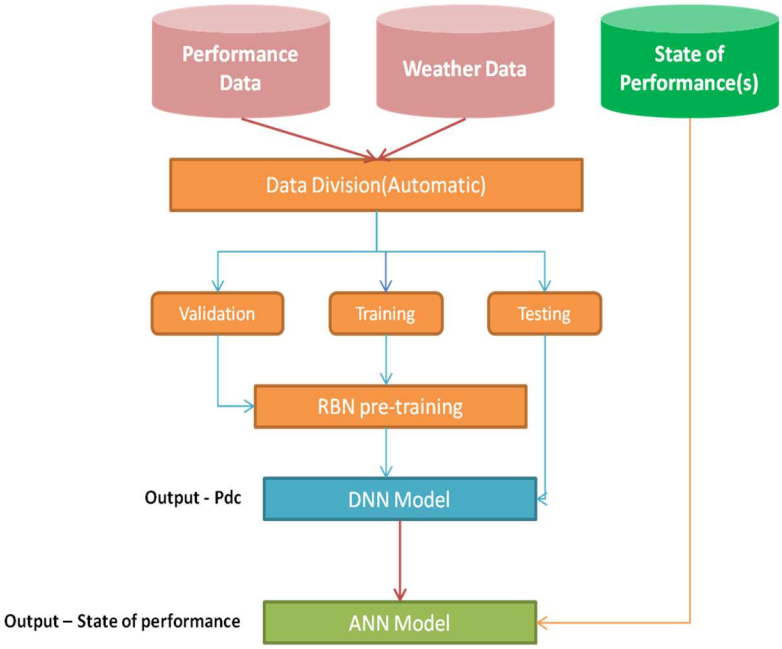

Figure 3.14 Overview of the Deep Neural Network Model.

CHAPTER FOUR: RECURRENT NEURAL NETWORK (RNN- LSTM) BASED FORECASTING OF PV BASED ISLANDED MICROGRID

4.1 Architecture and Problem Formulation

Forecasting techniques as mentioned in the literature have been investigated widely as in fig 4.1, in this article however, a robust technique of LSTM with comparison to SVM models have shown promising results [91]. Historically recorded and acquired Solar Data have been used in this experiment to implement LSTM and SVM models. National Renewable Energy Lab (NREL) has a software System Advisor Model (SAM) [93] to retrieve various historical data in regard to renewable resources.

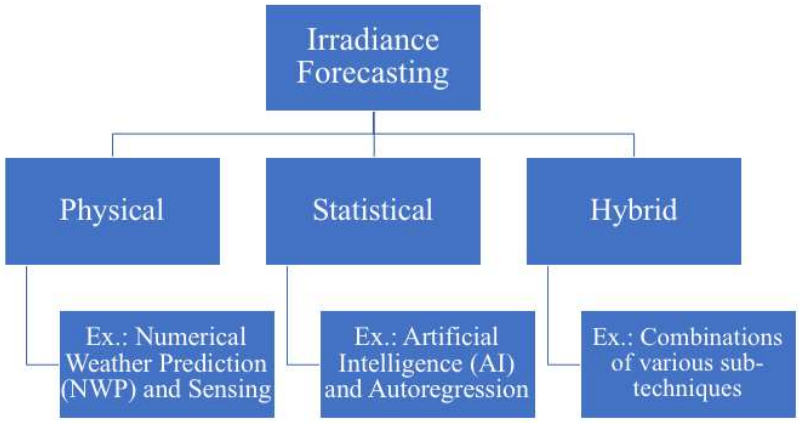

Figure 4.1 Solar Forecasting Categories.

In this work [91], Denver's Colorado solar (beam DNI, global GHI and diffuse DHI) irradiances data as shown in Figure 4.2. was selected to be investigated and associated. Beam Irradiance and a one PV module generated data were the main data parameter to be straggled in this paper. Input data modeled as a time sequence and is denoted as:

$$x_{1,t}\ , x_{2,t+1}\ , x_{3,t+2}\ , \ldots\ldots,\ x_{n,t+(n-1)} = x_{n,t}\ , \qquad x_{n,t} \in \mathbb{R} \tag{66}$$

Where x_n is the Irradiance value at step (n) at time (t).

Each input element is a real valued vector in which time stamped and labeled. The target sequence or the prediction output is:

$$y_t\ , y_{t+1}\ , y_{t+2}\ , \ldots\ldots, y_{t+(m-1)} = y_{m,t}\ , \qquad y_{t,m} \in \mathbb{R} \tag{67}$$

Where $y_{t,m}$ is the predicted solar data point sequence of values at step (m) and time (t).

The function of the prediction objective function is calculated based on the previous data and it is as follows:

$$Obj = \arg\min \sum_{n=1}^{m} \left[(x_{n,t}) - (y_{m,t})\right]^2 \tag{68}$$

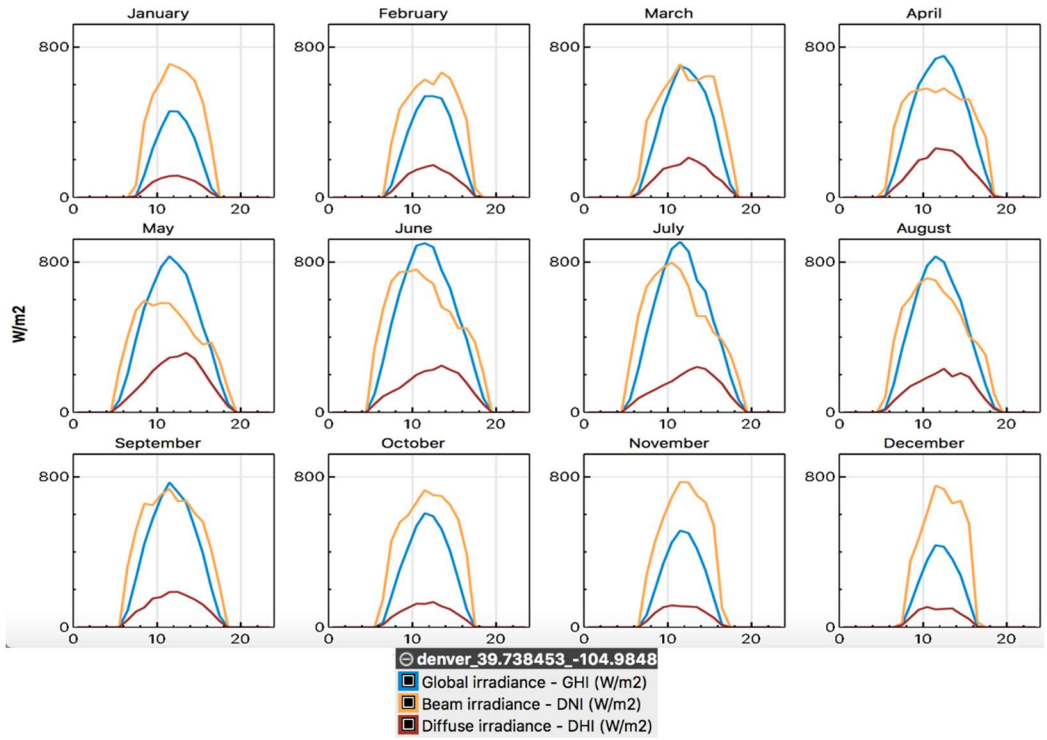

Figure 4.2 Annual average of Irradiance (GHI, DNI, DHI) Denver, CO (SAM)

4.1.1 Recurrent Neural Networks (RNNs)

In the recent years an enthused upbeat scheme by the abilities of the human being's brains, has shown indispensably beneficial outcomes. Prediction is one of those abilities that interests roughly every researcher in STEM. As a crucial part of the Artificial Neural networks, RNNs has emerged a powerful technique in various scientific fields as robust and efficient in high predicting accuracy. RNNs are generally a feedforward Neural Network unless the directed nodes are can be useful in short-term learning dependencies where data updated accordingly for better prediction accuracy.

Long Short Term Memory networks (LSTMs) [82] is a unique kind of RNNs where dependencies are prolonged which would help greatly in learning process effectiveness. It consists of five compulsory steps (input, forget, output, cell, state) [81], where those rudiments perform in reading, writing and removing fundamentally to all memory conditions. In typical RNNs, vanishing gradient descent is an issue; in contrast, LSTMs have overcome this issue, and this is one of the decisive reasons it is favorable.

The mathematical formulation of the hidden cell values (h_t) at time (t) for the current value of ($x_{n,t}$):

$$h_t = \lambda(W_{hx}^T * x_{n,t} + W_{hh}^T * h_{t-1} + b_h) \quad (69)$$

Where,

λ: is the activation function

W_{hx} : the weight matrix between hidden and input layers

W_{hh} : the recurrent weight matrix between the hidden and itself

b_h : bias parameter for h

T: is the transpose

Nearly in all typical feedforward multilayered neural networks, input is fed to neurons in a sequential way at the input layer. Next, the activation function will be multiplying the input to become a processed input for the next layer. Then, every hidden layer (h) neuron's output is multiplied by the connections weight matrices (W) and the bias term (b).

$$y_t = \lambda(W_{yh}^T * h_t + b_y) \quad (70)$$

Where,

λ: is the activation function

W_{yh} : the weight matrix between hidden and output layers

b_y : bias parameter for y

T: is the transpose

4.1.2 Support Vector Machines – Regression (SVRs):

SVMs [83] had been strongly presented in the research arena in the last decades for its useful usage in numerous statistical models. On the other hand, in recent years SVRs [83] have developed to be in a new face of SVMs. Hence, SVRs implement the same principles as SVMs in regard of classifications but in a different methodology. Taking advantage of regression, error is minimized given the idea of separating the hyperplane in order to widen the margin of tolerance.

$$y_t = f(x) = W * \beta(x) + b \quad (71)$$

Where,

x: input

y: output

W : is the weight vector

b : is Bias parameter

4.2 Exploratory Modeling and Analysis

By using the Artificial intelligence furthermost innovative tool to date, Python has proven to be a suitable tool for such demonstrating. In this section Data gathering, the proposed model details and Evaluation Metrics have been premeditated comprehensively utilizing the SAM [83] bulky data source. Supplementary, their results have been compared besides the results were drawn for better understanding, forecasting and predicting the Irradiance of Denver Colorado in the United states based on historical bulky data.

4.2.1 Input features:

Data was collected from the SAM application by NREL, where beam irradiance (W/m2) data and generated power for one PV module were obtained for the period from Jan 1st, 2018 to December 31st, 2018. More than 8700+ samples are assembled and investigated in this research.

4.2.2 Algorithm framework:

Three models as shown in figure 3, were performed on the input data in which raw data was normalized and divided into training and testing phases 80% and 20% respectively. The three models are Short Term Forecasting (STF) for prediction in hours, Medium Term Forecasting (MTF) for prediction in days and Long-Term Forecasting (LTF) for prediction in weeks. Python along with its major libraries on top of them is Keras-Tensorflow were used in this modeling with flexible epochs stipulations in which the

system only stops when there is no improvement in the prediction. The activation function that used in this model was sigmoid function.

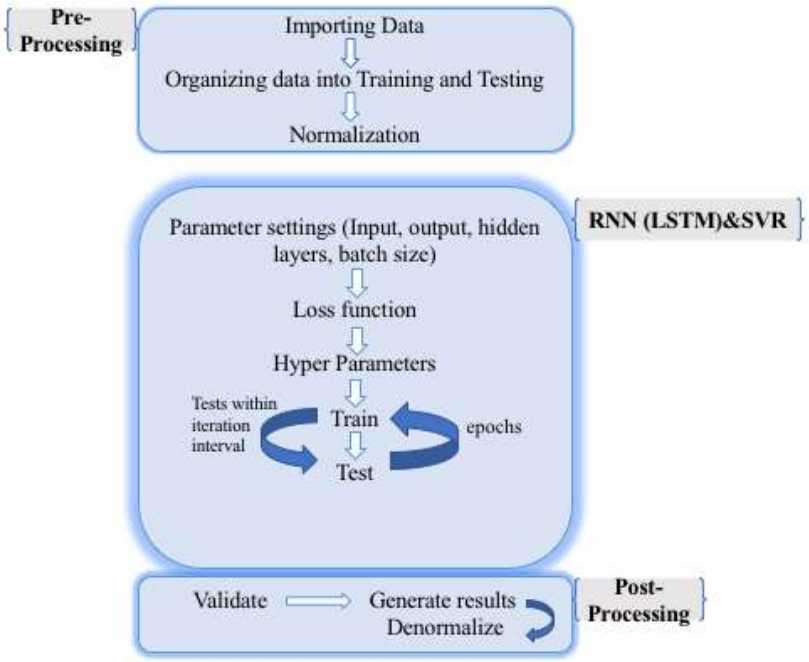

Figure 4.3 Proposed Architecture overview

4.2.3 Evaluation Metrics:

Measurement of the performance of any propositioned model is a necessary validation procedure to evaluate the outcome. Based on the raw data processing for several time apertures using the above-mentioned framework, a widely used techniques which is Root Squared Mean Error (RMSE):

$$RMSE = \sqrt{\frac{1}{n}\sum_{i=1}^{n}(x_i - y_i)^2} \quad (72)$$

Consequently, the performance of prediction and the coefficient of variation were implemented on each model and time frame:

$$CV = \frac{RMSE}{\mu} \tag{73}$$

Where,

x_n : input solar data

y_n : predicted output of solar

μ : average value

4.3 Results and Discussion

The model was trained on the aforementioned obtained data from NREL SAM system, thenceforward then data was tested broadly in the following two cases:

4.3.1 LSTM (case 1):

In this case, the system was modeled to be acquiring all the needed parameters files thenceforth train and test the obtained data. Additionally, the system was configured to be performing non-predefined epochs, in other words the algorithm would stop training and testing procedures only if the no noticeable improving into the classification are shown.

4.3.1.1 LSTM Short Term Forecasting (STF):

In this model, an hourly system was developed to predict the generated power based on the solar Irradiance on hourly bases. Generated power data was used, a one PV module was utilized in this experiment. The results of STF shown in table 1 and figure 4.4. It's obvious that LSTM has performed outstandingly by predicting the desired data in the STF.

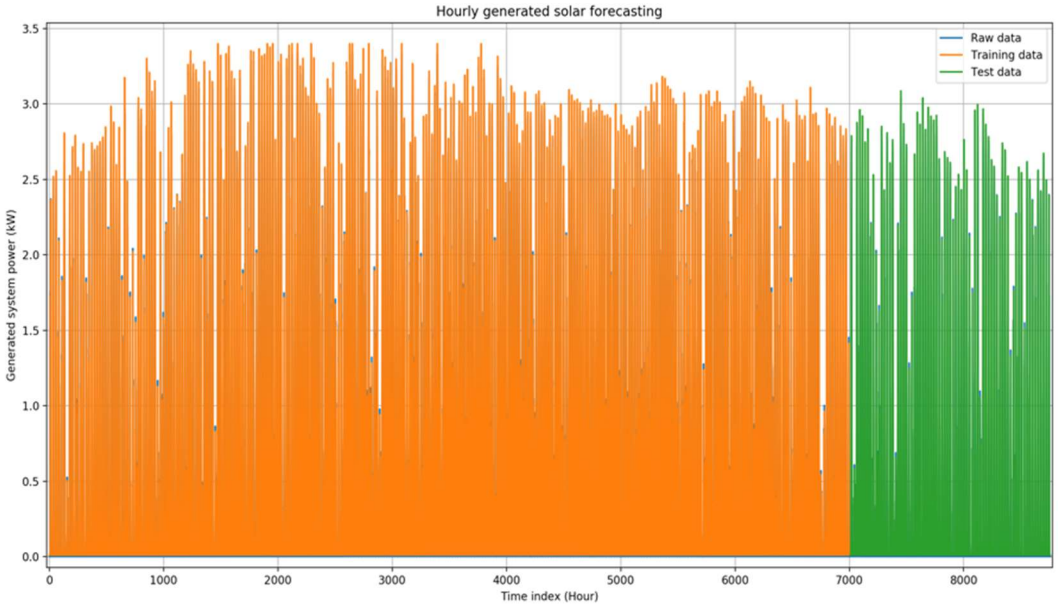

Figure 4.4 LSTM Hourly Forecasting Results

4.3.1.2 LSTM Medium Term Forecasting (MTF):

Daily predicted solar values were trained and tested. The rooted mean squared error and coefficient variations are calculated in table 1. Figures 4.5 & 4.6 shows the loss rate and variations illustrations.

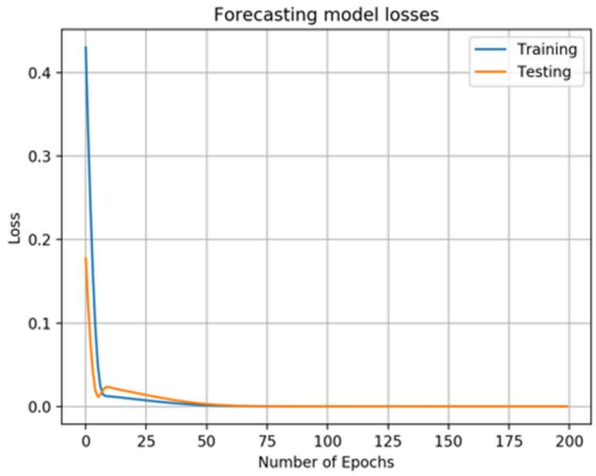

Figure 4.5 LSTM Daily model losses illustration

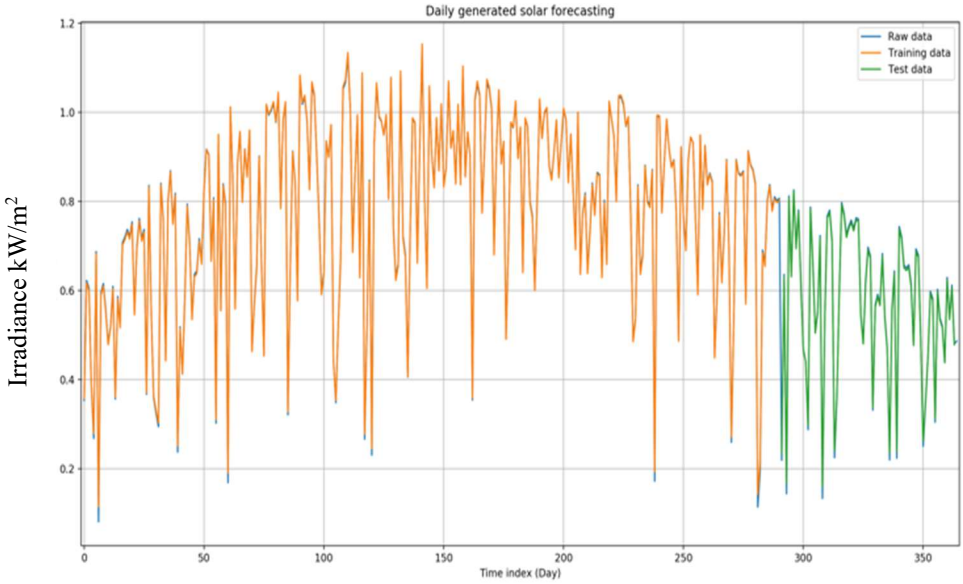

Figure 4.6 Forecasted data

4.3.1.3 LSTM Long Term Forecasting (LTF):

Here are the weekly values were considered in this model for a whole year. Accuracies and error values are shown in table 1 and illustrations of the resulted data illustrated n figures 4.7 & 4.8.

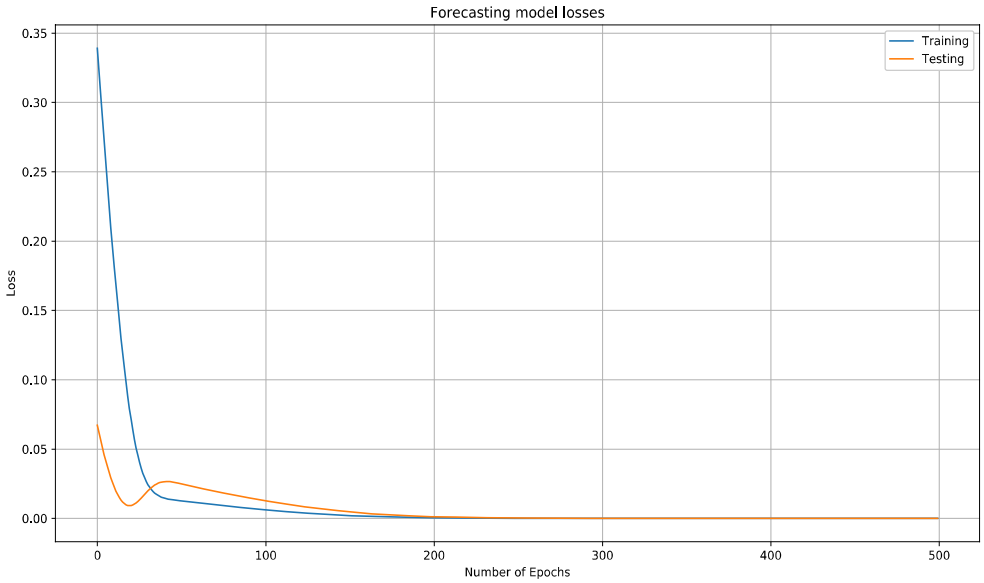

Figure 4.7 LSTM Weekly model losses

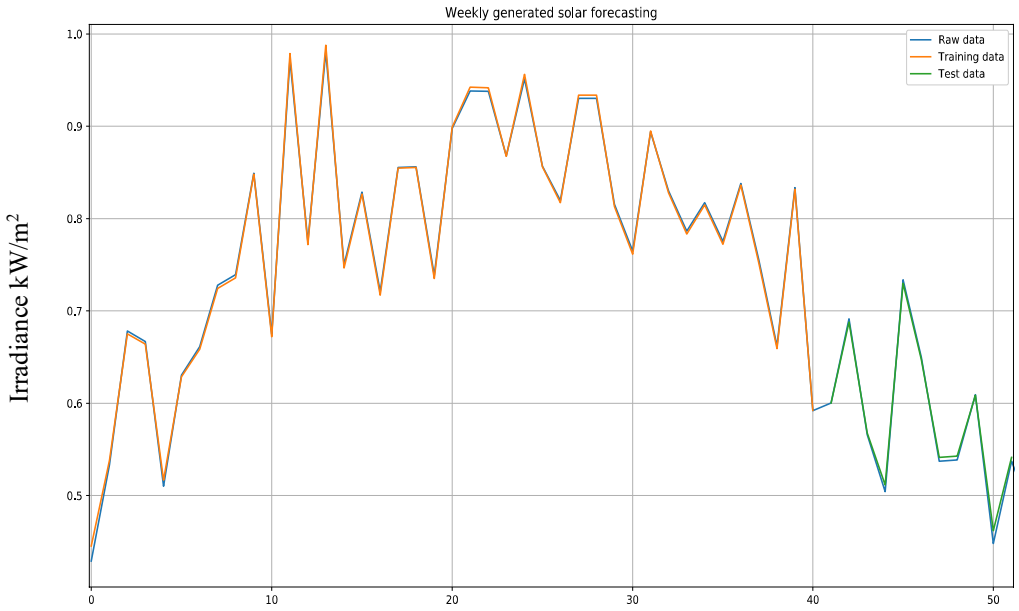

Figure 4.8 LSTM Weekly model Forecasting

4.3.2 SVR (case 2):

Support Vector Regression algorithm was sculpted and simulated using the sane parameters for LSTM. Similarly, Epochs were not predefined also where the system would be performing to gain the most of the obtained data. Three cases of STF, MTF and LTF were tested likewise in LSTM.

4.3.2.1 SVR Short Term Forecasting (STF):

SVR in STF which is hourly forecasting model, dissimilarly did not do well as expected since it doesn't have the ability of memory status as in LSTM. Especially in hourly forecasting where data get scattered in the SVR methodology. In this model, an hourly system was developed to predict the generated power based on the solar Irradiance on hourly bases. The module that was utilized in this experiment is consistent of multiple panels that add up roughly to 3.2 squared meters. Illustrations and RMSE, CV are demonstrated in figure 4.9 and table 4.1.

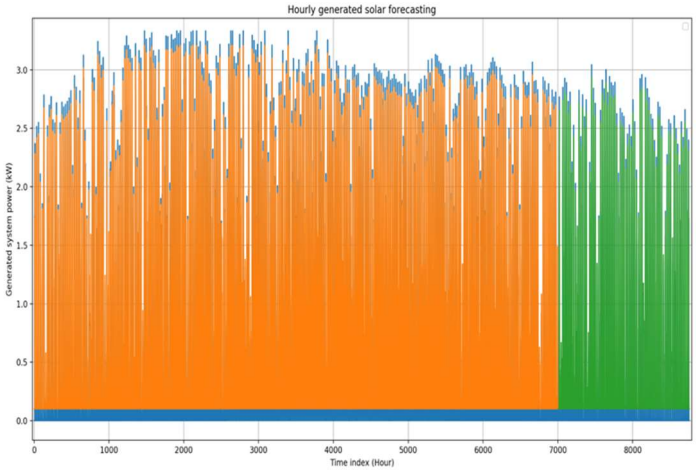

Figure 4.9 SVR Hourly forecasting data

4.3.2.2 SVR Medium Term Forecasting (MTF):

In this daily forecasting part of the modeling some progress in SVR for predicting was presented in comparison to STF, figure 4.10.

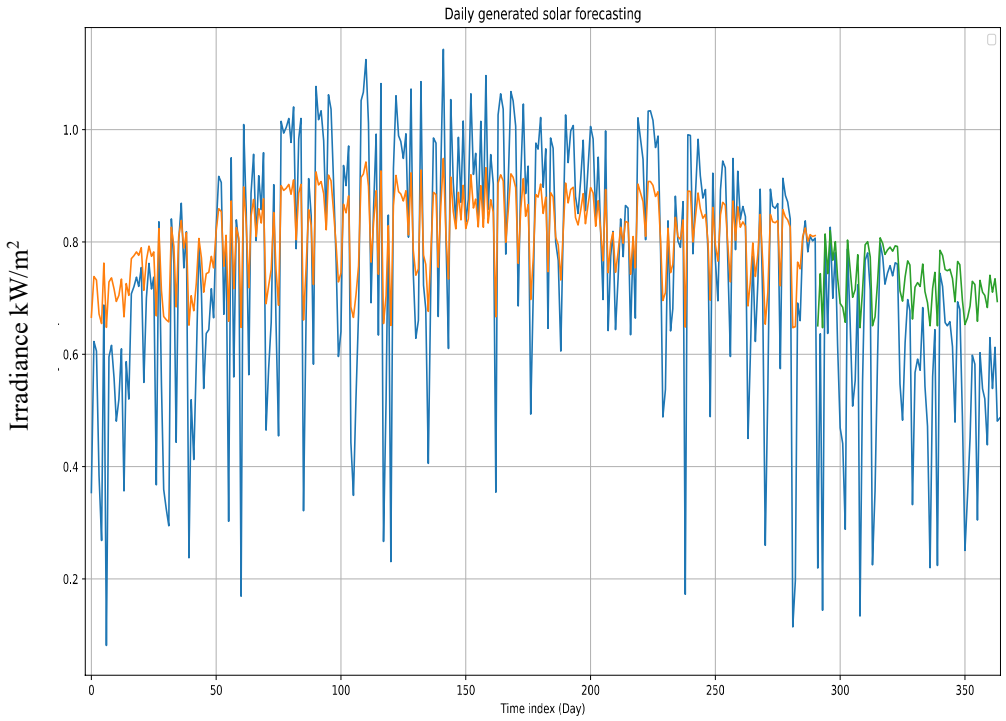

Figure 4.10 SVR Daily Forecasting data

4.3.2.3 Long Term Forecasting (LTF):

Weekly forecasted data was the best achievement of SVR in this architecture. Figure 4.11 and table 1 show the divergences and the error rates.

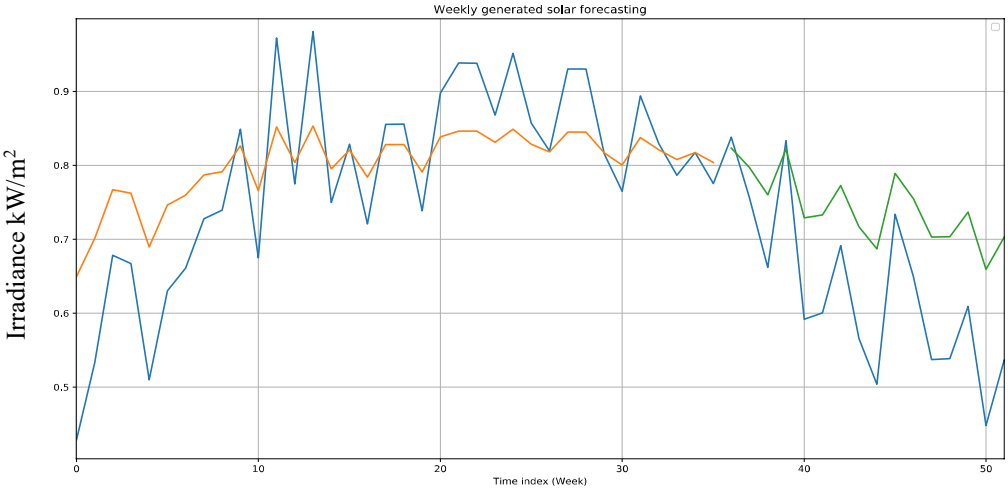

Figure 4.11 SVR Weekly forecasting data

Table 4.1 Numerical RMSE And CV Results of The Tested Models in the Proposed Algorithm

Model/Rate		CV (%)	RMSE (kW/h)	Mean (kW/h)
LSTM	STF	2.442	0.018	0.739
	MTF	1.020	0.008	0.739
	LTF	6.257	0.046	0.735
SVR	STF	53.817	0.398	0.740
	MTF	30.661	0.227	0.740
	LTF	22.320	0.165	0.741

It is obviously perceived from the diagrams of the fallouts and the table, that LSTM with all of its time boundaries, has accomplished way better than the conventional method of SVR. Specifically, the MTF class which was based on day to day forecasting procedure where accuracy is high. In STF, SVR executed poorly and it was its worst predictions in this model. In contrast to LSTM, LTF SVR achieved better only in comparison to its own time terms. It is worth more investigating and examining for understanding of such systems

CONCLUSION

The propositioned framework is concocted to be a robust and a comprehensive structure, and the tools which were used for developing hybrid algorithms in this research work have a common capability of vertical integration across the communication infrastructure (Mesh Networks) for extended applications besides exploiting a robust technique as Artificial Neural Network (ANNs). Hence, along with ANN versions of Deep Neural Networks (DNNs) which is also an effective scheme where it was efficiently implemented for accurate prediction modeling with 90+% rate. Thus, the deep neural network-based performance modeling system can be made more sophisticated to foresee possible issues underlying in the inverter or the distribution network from the data trend. Recurrent Neural Network (RNNs) submodule Long Short-Term Memory (LSTM) scheme was implemented and used to forecast Irradiance data on hourly, daily and weekly basis. Therefore, a comparison with another conventional methodology of Support Vector Machine – Regression technique. Obviously, LSTM shown optimal prediction results with higher accuracy giving its ability of memory significance notion through the process of training and testing where SVR was besieged with higher RMSE and CV.

Future directions would be attaining more investigations on more expended classification techniques and engaging monitoring of PV based smart and microgrid for smarter controlling. For example, EV charging stations can be integrated in the network as discussed in [79]. Thus, the current research effort provides a unique proposition of vertical integration which can be transformed into a new concept termed Internet of Microgrid (IoMG). Planning, monitoring, forecasting and operation form the core of smartgrids administration, and if intelligent tools intertwined with networks are being used as an integral part in each of these aspects, then it forms a holistic view of smartgrids. Furthermore, Blockchain is paving the way for new directions toward more reliable transactional power systems; in which the idea of prosumer would be very feasible in the soon future.

REFERENCES

[1] R. H. Lasseter and P. Paigi, "Microgrid: a conceptual solution," *2004 IEEE 35th Annual Power Electronics Specialists Conference (IEEE Cat. No.04CH37551)*, Aachen, Germany, 2004, pp. 4285-4290 Vol.6.

[2] R. E. P. N. for the 21st Century, "Renewables 2010 Global Status Report," Technical Report 2010, REN 21.

[3] M. A., A. M., "Micro Grid Technological Activities across the Globe: A Review", International Journal of Research and Reviews (IJRR) Applied Sciences, Volume 7, Issue 2, May '2011.

[4] M. F., H. N. K., "System Modeling and Online Optimal Management of a Microgrid with Battery Storage"", International Conference on Renewable Energies and Power Qualities, 4th issue, Oct '2011.

[5] L. X., D. Ch., "Control and Operation of DC Microgrid with Variable Generation and Energy Storage", IEEE Transactions on Power Delivery, volume 26, 4th issue, Oct '2011.

[6] M. P., T. W., "Optimization of Exchange of Electrical Energy between Microgrid and Electricity Utility Distribution Network", Modern Electric Power Systems, 2010 Proceedings of the International Symposium, September '2010.

[7] P. A. Madduri, J. Poon, J. Rosa, M. Podolsky, E. A. Brewer and S. R. Sanders, "Scalable DC Microgrids for Rural Electrification in Emerging Regions," in *IEEE*

Journal of Emerging and Selected Topics in Power Electronics, vol. 4, no. 4, pp. 1195-1205, December ‘2016.

[8] K. Salameh, “Digital Ecosystem for Better Management of Power Systems : An Application on Microgrids,” *Thesis Present. to Univ. Pau Adour Countries, Fr. fulfillment Requir. degree Dr. Philos. Syst. Eng. Autom.*, vol. 2017, no. cc.

[9] I. M. Moreno-garcia, E. J. Palacios-garcia, I. Santiago, V. P. López, and A. Moreno-munoz, “Performance Monitoring of a Solar Photovoltaic Power Plant using an Advanced Real-Time System,” no. 12013096, pp. 1–6, 2016.

[10] Z. Taif, M. M. Lafifi, and B. Boulebtateche, “Diagnosis of a Solar Power Plant using TS Fuzzy- based MultiModel approach,” *Int. Power Electron. Motion Control Conf. Expo.*, pp. 325–330, 2014.

[11] R. Setiabudy, B. S. Hartono, and Budiyanto, “Development energy management strategy to optimize battery operation in islanding microgrid using zero one integer programming,” *14th Int. Conf. QiR (Quality Res. QiR 2015 - conjunction with 4th Asian Symp. Mater. Process. ASMP 2015 Int. Conf. Sav. Energy Refrig. Air Cond. ICSERA 2015*, pp. 125–128, 2016.

[12] A. Almadhor, “Feedback-oriented intelligent monitoring of a storage-based solar photovoltaic (pv)-powered microgrid with mesh networks,” *Energies*, vol. 11, no. 6, 2018.

[13] “Digitalisation and Solar : Task Force Report,” Solar Power Europe Dec. 2017.

[14] T. Hiy., S. I., and K. K., “Neural Networks Based Estimation of Maximum Power Generation from PV Module Using Environmental Information,"*IEEE Transactions Ener. Convers.*, volume 12, no. 3, pp. 241-247, September 1997.

[15] A. Al-Amoudi and L. Zhang, “Application of radial basis function networks for solar array modelling and maximum powerpoint prediction,” *IET*, Generation, Transmissions and Distributions, volume 147, no. 5, pp. 310-316, Sep. 2000.

[16] A. Mellit, M. Menghanem, and M. Bendekhis, “Artificial neural network model for prediction solar radiation data: application for sizing stand-alone photovoltaic power system,” *IEEE Power Eng. Soc. Gen. Meet. 2005*, no. 2, p. 40–44 Vol. 1, 2005.

[17] J. L., W. F., X. Z., and C. Yan., “An Improved Photovoltaic Power Forecasting An Improved Photovoltaic Power Forecasting Model With the Assistance of Aerosol Index Data, ” *IEEE Trans. Sustain. Energy*, volume 6, no 2, pp. 434 - 442, May '2015.

[18] A. A., T. X. W., and B. R., “A Hybrid Algorithm for Short-Term Solar Power Prediction: Sunshine State Case Study,” *IEEE Trans. Sustain. Energy*, volume 8, no 2, pp. 582 – 591, April '2017.

[19] E. İzgi, A. Öztopal, B. Yerli, M. K. Kaymak, and A. D. Şahin, “Short–mid-term solar power prediction by using artificial neural networks,” *Sol. Energy*, vol. 86, no. 2, pp. 725–733, 2012.

[20] A. Yona, T. Senjyu, T. Funabashi, and C. H. Kim, “Determination method of insolation prediction with fuzzy and applying neural network for long-term ahead PV power output correction,” *IEEE Trans. Sustain. Energy*, vol. 4, no. 2, pp. 527–533, April 2013.

[21] A. Yona, T. Senjyu, A. Y. Saber, T. Funabashi, H. Sekine, and C. H. Kim, “Application of neural network to one-day-ahead 24 hours generating power forecasting for photovoltaic system,” *2007 Int. Conf. Intell. Syst. Appl. to Power Syst. ISAP*, pp. 1-6, 5-8 Nov. 2007.

[22] H. T. C. Pedro and C. F. M. Coimbra, “Assessment of forecasting techniques for solar power production with no exogenous inputs,” *Sol. Energy*, vol. 86, no. 7, pp. 2017–2028, 2012.

[23] R. H. Inman, H. T. C. Pedro, and C. F. M. Coimbra, “Solar forecasting methods for renewable energy integration,” *Prog. Energy Combust. Sci.*, vol. 39, no. 6, pp. 535–576, 2013.

[24] P. Vinay and M. A. Mathews, “Modelling and analysis of artificial intelligence based MPPT techniques for PV applications,” *2014 Int. Conf. Adv. Green Energy, ICAGE 2014*,, pp. 56–65, 17-18 Dec. 2014.

[25] Y. Su., S. Li, B. Li., X. Fu, M. Rame., and I. Jaith., "Artificial Neural Network for Control and Grid Integration of Residential Solar PV Systems," *IEEE Trans. Sustain. Ener.*, volume 8, no. 4, pp. 1484–1495, October 2017.

[26] S. P., F. M., and R. K., "Modelling of Soiled Photovoltaic Modules with neural networks and regression using particle size composition," *Solar Ener.*, volume 123, pp 116–126 , 2016.

[27] S. P., and, R. K., "Power prediction of soiled photovoltaic modules with neural networks (NN) using hybrid data clustering and division techniques," *Solar Ener.*, volume 133, 2016.

[28] A. Mel. et al. , "Modeling and simulation of a stand alone PV system using an adaptive artificial neural network (ANN) , a proposition for a new sizing procedure," *Renewable Ener.*, volume 32, no. 2, pp. 285 – 313, 2007.

[29] M. N. Akram and S. Lotfifard, "Modeling and Health Monitoring of DC Side of Photovoltaic Array," *IEEE Trans. Sustain. Energy*, vol. 6, no. 4, pp. 1245–1253, Oct. 2015.

[30] X. Huang, S. H. Hong, and Y. Li, "Hour-Ahead Price Based Energy Management Scheme for Industrial Facilities," *IEEE Trans. Ind. Informatics*, vol. 13, no. 6, pp. 2886–2898, 2017.

[31] S. Khomfoi and L. M. Tolbert, “Fault diagnostic system for a multilevel inverter using a neural network,” *IEEE Trans. Power Electron.*, vol. 22, no. 3, pp. 1062–1069, May 2007.

[32] M. R., N. A., H. Le-M., S. H., Y. C., and N. M. K., “A Critical Analysis of Research Potential, Challenges and Future Directives in Industrial Wireless Sensor Networks, ” *IEEE Communication Survey Tutorials*, volume 20, no. 1, pp. 39-75, 2018.

[33] D. Anderson *et al.*, “GridCloud: Infrastructure for Cloud-based Wide Area Monitoring of Bulk Electric Power Grids,” *IEEE Trans. Smart Grid*, vol. , no. 99, 2018.DOI: 10.1109/TSG.2018.2791021

[34] X. Wang, S. Member, Y. Pi, W. Mao, and H. Huang, “Network Coordinated Power Point Tracking for Grid-Connected Photovoltaic Systems,” *IEEE J. Sel. areas Commun.*, vol. 32, no. 7, pp. 1425–1440, July 2014.

[35] Y. Ju, W. Wu, B. Zhang, and H. Sun, “An extension of FBS three-phase power flow for handling PV Nodes in active distribution networks,” *IEEE Trans. Smart Grid*, vol. 5, no. 4, pp. 1547–1555, July 2014.

[36] A. Almadhor, “Automatic PV Performance Diagnosis Through Inverter Data Using DNN Architecture” *IEEE ROPEC, Ixtapa Mexico,* Nov 2018.

[37] M. A. Eltawil and Z. Zhao, “Grid-connected photovoltaic power systems: Technical and potential problems-A review,” *Renew. Sustain. Energy Rev.*, vol. 14, no. 1, pp. 112–129, 2010.

[38] H. Farhangi, “The path of the smart grid,” *IEEE Power Energy Mag.*, vol. 8, no. 1, pp. 18–28, 2010.

[39] Y. Yan, Y. Qian, H. Sharif, and D. Tipper, “A Survey on Smart Grid Communication Infrastructures : Motivations , Requirements and Challenges A Survey on Smart Grid Communication Infrastructures : Motivations , Requirements and Challenges,” *IEEE Commun. Surv. tutorials*, vol. 15, no. 1, pp. 1–16, 2013.

[40] V. K. Sood, D. Fischer, J. M. Eklund, and T. Brown, “Developing a communication infrastructure for the smart grid,” *2009 IEEE Electr. Power Energy Conf. EPEC 2009*, vol. 4, pp. 1–7, 2009.

[41] G. W. Chang *et al.*, “Modelling and simulation for INER AC microgrid control,” *IEEE Power Energy Soc. Gen. Meet.*, vol. 2014–Octob, no. October, 2014.

[42] M. M. Rana and L. Li, “Kalman Filter Based Microgrid State Estimation Using the Internet of Things Communication Network,” *2015 12th Int. Conf. Inf. Technol. - New Gener.*, pp. 501–505, 2015.

[43] A. Khalil and K. Ateea, “Modelling and Control of Photovoltaic-Based Microgrid,” *Int. J. Renew. Energy Res.*, vol. 5, no. 3, pp. 826–835, 2015.

[44] Y. S. Bhavsar, P. V. Joshi, and S. M. Akolkar, “Simulation of Microgrid with energy management system,” *Int. Conf. Energy Syst. Appl. ICESA 2015*, no. Icesa, pp. 592–596, 2016.

[45] Q. I. Ali, A. Abdulmaowjod, and H. M. Mohammed, “Simulation &performance study of wireless sensor network (WSN) using MATLAB,” *Energy, Power Control (EPC-IQ), 2010 1st Int. Conf.*, pp. 307–314, 2010.

[46] F. Ye, S. Member, Y. Qian, S. Member, R. Q. Hu, and S. Member, “Energy Efficient Self-Sustaining Wireless Neighborhood Area Network Design for Smart Grid,” vol. 6, no. 1, pp. 220–229, 2015.

[47] E. Spanò, L. Niccolini, S. Di Pascoli, and G. Iannaccone, “Last-meter smart grid embedded in an internet-of-things platform,” *IEEE Trans. Smart Grid*, vol. 6, no. 1, pp. 468–476, 2015.

[48] T. le F. Kristensen, R. L. Olsen, J. G. Rasmussen, and H.-P. Schwefel, “Information access for event-driven smart grid controllers,” *Sustain. Energy, Grids Networks*, vol. 13, pp. 78–92, 2018.

[49] D. Anderson *et al.*, “GridCloud: Infrastructure for Cloud-based Wide Area Monitoring of Bulk Electric Power Grids,” *IEEE Trans. Smart Grid*, vol. 3053, no. c, 2018.

[50] J. Choi, Y. Shin, M. Choi, W.-K. Park, and I.-W. Lee, “Robust Control of a Microgrid Energy Storage System using Various Approaches,” *IEEE Trans. Smart Grid*, vol. 7, no. 4, pp. 1–1, 2018.

[51] S. A. M. Al-Barazanchi and A. M. Vural, “Modeling and intelligent control of a stand-alone PV-Wind-Diesel-Battery hybrid system,” *2015 Int. Conf. Control Instrum. Commun. Comput. Technol. ICCICCT 2015*, pp. 423–430, 2016.

[52] M. D. Phung, M. De La Villefromoy, and Q. Ha, “Management of solar energy in microgrids using IoT-based dependable control,” *2017 20th Int. Conf. Electr. Mach. Syst. ICEMS 2017*, 2017.

[53] S. Frey, A. Diaconescu, D. Menga, and I. Demeure, “A holonic control architecture for a heterogeneous multi-objective Smart Micro-Grid,” *Int. Conf. Self-Adaptive Self-Organizing Syst. SASO*, pp. 21–30, 2013.

[54] M. S. Bisht and Sathans, “Fuzzy based intelligent frequency control strategy in standalone hybrid AC microgrid,” *2014 IEEE Conf. Control Appl. CCA 2014*, pp. 873–878, 2014.

[55] S. Kr. Tiwari, B. Singh, and P. K. Goel, “Design and Control of Micro-Grid fed by Renewable Energy Generating Sources,” *IEEE Trans. Ind. Appl.*, vol. 9994, no. c, pp. 1–9, 2018.

[56] Y. Mi, H. Zhang, S. Member, Y. Fu, and C. Wang, “Intelligent Power Sharing of DC Isolated Microgrid Based on Fuzzy Sliding Mode Droop Control,” *IEEE Trans. Smart Grid*, vol. 3053, no. c, 2017.

[57] A. P. Grilo, P. Gao, W. Xu, and M. C. De Almeida, “Load monitoring using distributed voltage sensors and current estimation algorithms,” *IEEE Trans. Smart Grid*, vol. 5, no. 4, pp. 1920–1928, 2014.

[58] P. Chakraborty, E. Baeyens, and P. P. Khargonekar, “Distributed control of flexible demand using proportional allocation mechanism in a smart grid: Game theoretic

interaction and price of anarchy," *Sustain. Energy, Grids Networks*, vol. 12, pp. 30–39, 2017.

[59] A. U. Krismanto, N. Mithulananthan, and O. Krause, "Sustainable Energy , Grids and Networks Stability of Renewable Energy based Microgrid in Autonomous Operation," *Sustain. Energy, Grids Networks*, vol. 13, pp. 134–147, 2018.

[60] B. McMillin and T. Roth, "Cyber-Physical Security and Privacy in the Electric Smart Grid," *Synth. Lect. Inf. Secur. Privacy, Trust*, vol. 9, no. 2, pp. 1–64, 2017.

[61] Y. He, G. J. Mendis, and J. Wei, "Real-Time Detection of False Data Injection Attacks in Smart Grid: A Deep Learning-Based Intelligent Mechanism," *IEEE Trans. Smart Grid*, vol. 8, no. 5, pp. 2505–2516, 2017.

[62] T. Khatib and W. Elmenreich, "Novel simplified hourly energy flow models for photovoltaic power systems," *Energy Convers. Manag.*, vol. 79, pp. 441–448, 2014.

[63] S. X. Chen, H. B. Gooi, and M. Q. Wang, "Sizing of energy storage for micro grids," *IEEE Trans. Smart Grid*, vol. 3, no. 1, pp. 142–151, 2012.

[64] A. H. Hubble and T. S. Ustun, "Composition, placement, and economics of rural micro grids for ensuring sustainable development," *Sustain. Energy, Grids Networks*, vol. 13, pp. 1–18, 2018.

[65] https://openweathermap.org

[66] www.pvsyst.org

[67] A. Tajer, S. Kar, H. V. Poor, and S. Cui. Distributed joint cyber attack detection and state recovery in smart grids. In *Smart Grid Communications (SmartGridComm), IEEE International Conference on*, pages 202–207, 2011.

[68] K. H. Hussein, "Maximum photovoltaic power tracking: an algorithm for rapidly changing atmospheric conditions," *IEE Proc. - Gener. Transm. Distrib.*, vol. 142, no. 1, p. 59, Jan. 1995.

[69] S. Mekhilef, R. Saidur, and M. Kamalisarvestani, "Effect of dust, humidity and air velocity on efficiency of photovoltaic cells," *Renew. Sustain. Energy Rev.*, vol. 16, no. 5, pp. 2920–2925, June 2012.

[70] M. T. Hagan and M. B. Menhaj, "Training feed forward networks with the Marquardt algorithm" *IEEE Trans. Neural Networks*, vol. 5, no. 6, pp. 2–6, Nov.19

[71] Huang Yi, Sun Shiyu, Duan Xiusheng and Chen Zhigang, "A study on Deep Neural Networks framework," 2016 IEEE Advanced Information Management, Communicates, Electronic and Automation Control Conference (IMCEC), Xi'an, 2016, pp. 1519-1522.

[72] T. Dragičević, H. Pandžić, D. Škrlec, I. Kuzle, J. M. Guerrero, and D. S. Kirschen, "Capacity Optimization of Renewable Energy Sources and Battery Storage in an Autonomous Telecommunication Facility," *IEEE Trans. Sus. Energy*, vol. 5, no. 4, pp. 1367–1378, 2014.

[73] S. Prasad and V. K. Dulla Mallesham, “Multi-objective hybrid estimation of distribution algorithm-interior point method-based meter placement for active distribution state estimation,” *IET Gener. Transm. Distrib.*, vol. 12, no. 3, pp. 767–779, 2018.

[74] C. M. Huang, S. J. Chen, S. P. Yang, Y. C. Huang, and ..., “Capacity optimisation for an SAMS considering LCOE and reliability objectives,” *IET Renew. Power ...*, 2018.

[75] F. Hussain, Y. Hassan, S. Hossen, and S. Choudhury, “System Capacity Maximization with Efficient Resource Allocation Algorithms in D2D Communication,” *IEEE Access*, vol. 3536, no. c, pp. 32409–32424, 2018.

[76] Y. Hayashi and J. Matsuki, “Loss Minimum Configuration of Distribution System Considering N-1 Security of Dispersed Generators,” *IEEE Trans. Power Syst.*, vol. 19, no. 1, pp. 636–642, 2004.

[77] H. Long, M. Eghlimi, and Z. Zhang, “Configuration Optimization and Analysis of a Large Scale PV/wind System,” *IEEE Trans. Sustain. Energy*, vol. 3029, no. c, pp. 1–1, 2016.

[78] S. Bhattacharjee, A. Bhattacharya, and S. Sharma, “Grey wolf optimisation for optimal sizing of battery energy storage device to minimise operation cost of microgrid,” *IET Gener. Transm. Distrib.*, vol. 10, no. 3, pp. 625–637, 2016.

[79] A. Kavousi-Fard, and A. Khodaei, “Efficient Integration of Plug-in Electric Vehicles via Reconfigurable Microgrids,” Energy, 2016.

[80] “RTO,” 2016.

[81] A. Almalaq and G. Edwards, “Comparison of Recursive and Non-Recursive ANNs in Energy Consumption Forecasting in Buildings,” *2019 IEEE Green Technol. Conf.*, pp. 1–5, 2019.

[82] S. Hochreiter and J. J. Urgen Schmidhuber, “Long Short-Term Memory” Neural Computation, 1997.

[83] A. J. Smola, B. Sch¨olkopf, and S. Sch¨olkopf, “A tutorial on support vector regression *,” Kluwer Academic Publishers, 2004.

[84] S. E. Haupt *et al.*, “Building the Sun4Cast System: Improvements in Solar Power Forecasting,” *Bull. Am. Meteorol. Soc.*, 2017.

[85] S. Mishra and P. Palanisamy, “Multi-time-horizon Solar Forecasting Using Recurrent Neural Network,” *2018 IEEE Energy Convers. Congr. Expo. ECCE 2018*, pp. 18–24, 2018.

[86] A. Mellit and A. M. Pavan, “A 24-h forecast of solar irradiance using artificial neural network: Application for performance prediction of a grid-connected PV plant at Trieste, Italy,” *Sol. Energy*, vol. 84, no. 5, pp. 807–821, 2010.

[87] D. Yang, “A guideline to solar forecasting research practice: Reproducible, operational, probabilistic or physically-based, ensemble, and skill (ROPES),” *J. Renew. Sustain. Energy*, vol. 11, no. 2, p. 22701, Mar. 2019.

[88] M. Negnevitsky, C. W. Potter, S. Member, and M. Negnevitsky, “Very Short-Term Wind Forecasting for Tasmanian Power Generation Very Short-Term Wind Forecasting for Tasmanian Power Generation,” vol. 21, no. October, pp. 965–972, 2015.

[89] P. Mathiesen and L. Spiegel, “Final Project Report Evaluation of Numerical Weather Prediction for Solar,” *Sol. Energy*, vol. 85, pp. 967–977.

[90] J. Polo, L. F. Zarzalejo, and L. Ramírez, “Solar Radiation Derived from Satellite Images BT - Modeling Solar Radiation at the Earth’s Surface: Recent Advances,” V. Badescu, Ed. Berlin, Heidelberg: Springer Berlin Heidelberg, 2008, pp. 449–462.

[91] A. Almadhor, M. Matin and D. Gao “Recurrent Neural Network (RNN-LSTM) Forecasting of PV based islanded Micorgrid” *SPIE, San Diego, CA, Aug 2019.*

[92] A. Zendehboudi, M. A. Baseer, and R. Saidur, “Application of support vector machine models for forecasting solar and wind energy resources: A review,” *J. Clean. Prod.*, vol. 199, no. August, pp. 272–285, 2018.

[93] SAM, “System Advisor Model” *NREL*. [Online]. Available: https://sam.nrel.gov.

[94] M. R., N. A., H. Le-M., S. H., Y. C., and N. M. K., “A Critical Analysis of Research Potential, Challenges and Future Directives in Industrial Wireless Sensor Networks,” *IEEE Communication Survey Tutorials*, vol. 20, no. 1, pp. 39-75, 2018.

[95] D. Anderson *et al.*, “GridCloud: Infrastructure for Cloud-based Wide Area Monitoring of Bulk Electric Power Grids,” *IEEE Trans. Smart Grid*, vol. , no. 99, 2018.DOI: 10.1109/TSG.2018.2791021.

[96] X. Wang, S. Member, Y. Pi, W. Mao, and H. Huang, “Network Coordinated Power Point Tracking for Grid-Connected Photovoltaic Systems,” IEEE J. Sel. areas Commun., vol. 32, no. 7, pp. 1425–1440, July 2014.

[97] Y. Ju, W. Wu, B. Zhang, and H. Sun, “An extension of FBS three-phase power flow for handling PV Nodes in active distribution networks,” IEEE Trans. Smart Grid, vol. 5, no. 4, pp. 1547–1555, July 2014.

[98] S. F. Bush; S. Goel; G. Simard, "IEEE Vision for Smart Grid Communications: 2030 and Beyond Roadmap," in IEEE Vision for Smart Grid Communications: 2030 and Beyond Roadmap , vol., no., pp.1-19, 3 Sept. 2013

[99] J. Jiang and Y. Qian, “Distributed communication architecture for smart grid applications”, IEEE Communications Magazine, vol. 54, no. 12, pp. 60-67, Dec. 2016.

[100] N. Kolokotronis, A. Katsiotis and N. Kalouptsidis, “Secretly pruned convolutional codes: Security analysis and performance results”, IEEE Trans. on Information Forensics and Security, vol. 11, no. 7, pp. 1500- 1514, July 2016.

[101] N. Shlezinger, D. Zahavi, and Y. Murin, “The secrecy capacity of Gaussian MIMO channels with finite memory”, to appear in IEEE Trans. on Information Theory.

[102] K. Ntemos, N. Kolokotronis and N. Kalouptsidis, “Using trust to mitigate malicious and selfish behavior of autonomous agents in CRNs,” 2016 IEEE 27th Annual International Symposium on Personal, Indoor, and Mobile Radio Communications (PIMRC), Valencia, 2016, pp. 1-7.

[103] J. A. Tropp and S. J. Wright, “Computational method for sparse solution of linear inverse problems”, Proceedings of IEEE, vol. 98, no. 6, pp. 948-958, June 2010.

[104] Z. Erkin, J. R. Troncoso-pastoriza, and R. L. Lagendijk, “Privacy-preserving data aggregation in smart metering systems: an overview”, IEEE Signal Processing Magazine, vol. 30, no. 2, pp. 75-86, Mar. 2013.

APPENDIX

$$\boldsymbol{\sigma} = \sqrt[\perp]{\mathbf{1} - \mathrm{e}^{\mathbf{2}}}$$

$$\boldsymbol{\varepsilon} = \boldsymbol{\nu\eta\gamma}\sqrt{\boldsymbol{\Sigma\pi}}\frac{\boldsymbol{v}}{\dot{\boldsymbol{z}}}$$

Elongated Literature and Motivations:

21st century is experiencing rapid technological developments in numerous areas to facilitate sustainable living. Renewable energy proliferation and Internet of Things are the two of many such areas, where significant progress is being achieved. With the increase in the intensity of renewable proliferation and its injection into utility grid, monitoring the assets that produce the energy and continuously evaluating the parameters (climatic) that dictate the performance is becoming increasingly important [37]. Researchers predict the transformation of normal electric grids into smart, next generation electric grid with renewable generation sources that will inevitably have the intersection of electrical as well as communication systems [38]. The grid will be a conglomeration of forward compatible hardware and software technologies to address evolving energy access patterns. These next generation grids, with the proliferation of digital infrastructure to improve financial and operational self-reliance, slowly transition into intertwining of communication infrastructure to the electrical infrastructure compulsory. The combination of electrical and communication system as shown in Fig.1. in the energy infrastructure, will enable functions based on the motivation of grid, like online monitoring, demand side

management, control along with critical functions like troubleshooting an event and its immediate reporting [39]. This interesting and apparent intersection of electrical and communication systems will expose a new horizon of opportunities to lead the energy revolution.

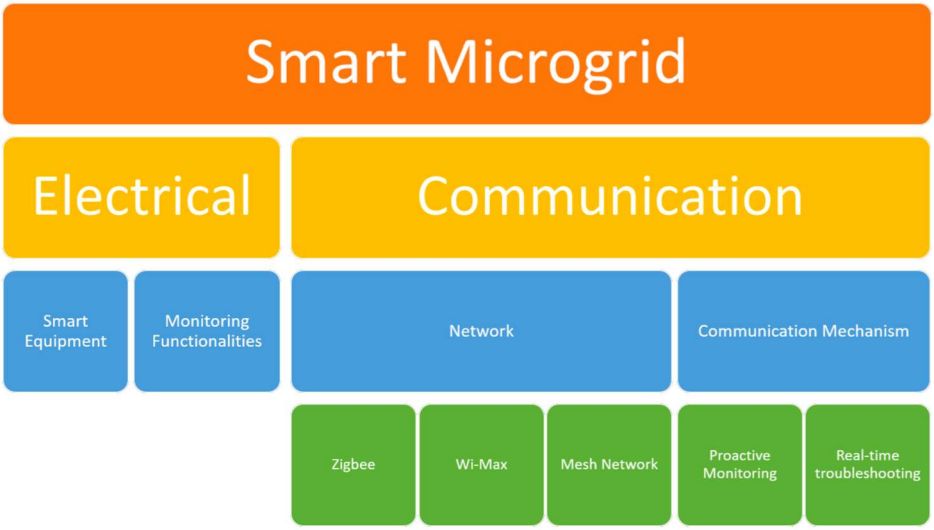

Fig.1. Intersection of Electrical and Communication Infrastructure - Root of Digitalization.

Sood et al. [40] developed a WiMax (worldwide interoperability for microwave access)-based smartgrid communication network for monitoring distributed energy generation sources. In a similar work [41], a grid-connected AC microgrid is simulated using the Simulink tool with basic communication infrastructure and a control strategy to optimize the performance in the grid is discussed. Masud and Li [42] developed and analyzed Internet of Things (IoT) based communication network for monitoring multiple distributed

energy sources using Kalman filter based state estimation of the microgrid. In [43][44], an IoT-based energy management system in microgrids for improving efficiency is proposed and studied in the context of PV generation systems, while a similar energy management system in a *PV*/wind hybrid microgrid is simulated in [45][46] using Simulink. A self-sustaining wireless neighborhood area network is designed in [47] for transmitting power grid sensing and measuring status as well as the control messages. While Spano et al. [48] included individual energy meters into the communication network to design a holistic model for smartgrid monitoring. Kristensen et al. [49] developed information access schemes between remote assets and controller, which are activated only when certain voltage thresholds are at any measurement point in the grid.

A dedicated communication network is needed to monitor the performance of individual plant or microgram for streamlining operations and decision making in [50]. The

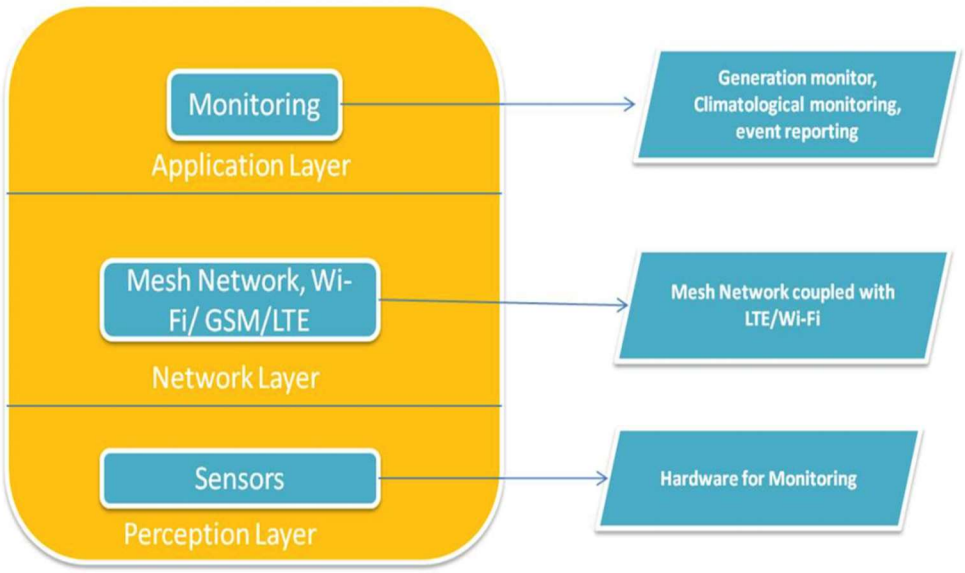

Fig.2. Layers of the communication network [14].

infrastructure is divided into layers as shown in Fig.2.

ANN based models widely expended for accurate power prediction and performance evaluation in these power plants. For example, the reports published by Solar Power Europe [51], emphasize the importance of ANN based tools to address the issues in renewable energy based powered smartgrid or microgrid. Solar resources availability are circumscribed and in need of an precise modelling for power prediction, which includes climatic conditions similar to wind, temperature, irradiance, humidity and soiling.

Research work reported in [52], predicted highest power harvest by implementing data input of weather elements into artificial neural networks techniques. In a similar research work described in [53], a proposal of radial basis function (RBF) was constructed neural network configuration to simulate PV solar arrays in a power plant. Experiments were carried out to predict solar radiation data using ANN models [54-58] to estimate power production of a PV system for a given duration.A day-ahead irradiance forecast is reported in [59] and [60], a comparison of different forecasting techniques was investigated in [61]. ANN model was used in [62] and [63] to predict the production of power of a PV system under dusty environmental conditions. Recent contributions use ANN models to achieve maximum power point (MPP) operations of a PV system [64], control and grid integration for residential solar PV operations [65] and adaptive ANN models for standalone PV systems [66]. Other applications of ANN models include health monitoring of PV arrays [67], hour ahead forecast of energy price in industries [68] and fault diagnostics of multilevel inverter used in these power-generating plants [69].

With the advent of fourth industrial revolution, the intersection of electrical and communication networks for monitoring and control of utility level infrastructure seems inevitable [70]. Researchers designed and developed communication architecture intertwined with PV generation systems like micro grid [71], grid-connected PV plants [72] and distributed solar power generation systems [73]. In [38], IEEE smartgrid

communication vision document outlines the necessity of communication intertwined with microgrid in the following ways:

A. **Power entropy:** Distributed and renewable generation in particular should remain synchronized with the main ac power frequency; maintaining frequency synchronization is a challenge requiring communication related to the inertia/momentum of the distributed/renewable generators. Figure 3 shows a simple communication network and equipment infrastructure for microgrid technologies for renewable integration. In addition, power generation for renewables is subject to potentially high entropy weather variations whose communication requirements are proportional to the entropy.

B. **Power area or density (dispersal/aggregation):** The area of power control can be from a large wind farm to the inverter control for a domestic photovoltaic system over a distribution system of today's power grid architecture.

C. **Power efficiency:** Maintaining the power factor within tighter bounds will require more communication.

D. **Amount of power drives latency:** As an example, protection mechanisms for distributed generation will require communication proportional to the amount of power similar to a time-current characteristic curve.

As the number of devices that participate in smart microgrids increases, the relevant smart operations are increasingly adopting a decentralized approach [74], rather than a

centralized one, leading to a subsequent increase in vulnerability and security risks of transmissions. Accomplishing improved protection, reliability and privacy, transmission schemes should be capable of detecting and handling eavesdroppers and malicious behavior [75]. The adopted schemes could utilize ideas from information theory (such as the notion of secrecy capacity [76]), multi-agent approaches [77] and game-theoretic

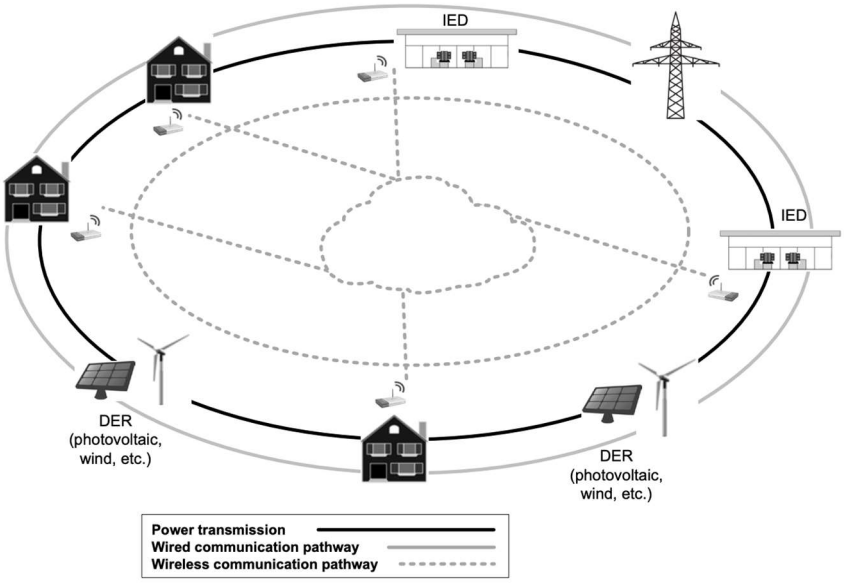

Fig.3. Micro-grids, consisting of DERs interconnected via the electricity grid and corresponding IEDs interconnected via the communication network.

modeling, while taking into account the constraints that are imposed, e.g, by critical microgrid operations (e.g., power balance control) with low latency requirements. For energy management and demand response purposes, the power consumption signals of the

domestic appliances of multiple houses are gathered at a remote concentration center for supporting decision making procedures [78]. The amount of data, however, could be excessive which could exhaust the available resources of the communication infrastructure, meaning that compression techniques should be employed. Sparse coding and dictionary learning algorithms [79] can lead to novel compression techniques, which are particularly suited to the considered consumption signals. It is interesting to point out that such techniques are compatible with techniques that are proposed for the problem of the so-called non-intrusive load monitoring [80].

It can be summarized that the protagonist of communication systems has been a crucial part to be integrated for microgrids to be enhanced and better performing. It is very obvious that the fluctuating nature in microgrids has instigated power generation sundry curbs. Solar and wind generation are volatile and power output can shift very hasty depending on instantaneous climatic transformation [81]. Such fluctuation would effect power management, distribution and voltage control [82]. Thus, countless management issues or even instable events can arise vastly in such fluctuating environment where power can excessive or distributed generations and large loads are not informed of dysconnectivity.

Artificial Neural Networks (ANNs) are mostly expended for accurate modeling prediction in these fields. For example, the irradiance was predicted using neural networks with different meteorological parameters in [83-90] while different artificial neural network models to predict the radiation data are compared in [91]. The power output of a solar PV

panel depends on factors like irradiance, orientation, tilt angle, surface degradations etc. and many research works have used fuzzy logic and similar mathematical tools to model power output with these factors. The power profile of grid connected PV modules is predicted using artificial neural networks as discussed in [92] while a new approach based on ANN is used to predict the power output in Indonesia is proposed in [93]. A non-parametrical model is developed using numerical weather forecast methods to predict the power output of a solar module in [94] and an optimum design of a neural tree is proposed in [95]. Different approaches based on neural networks have also been used in [96] and [97] to predict the power output of a PV module. The effect of tilt angle on the power output of the panel is considered in [98] and a neural network is developed to predict the power output. However it was in [99], the losses occurring on a PV module have been modelled and the power output is predicted with respective to the loss factors. These neural networks have also been finding many real life applications, especially in the growing field of photovoltaic operations [100]. Starting from solar cell [101], standalone PV modules [102] , MPPT [103] and power output [104] neural networks are being used to effectively model the respective phenomena. Hence, using ANN simplifies the characterization and strengthens the resolve of modelling PV power generation ecosystem.

List of Selected Publications:

- **Ahmad Almadhor**, "Feedback-Oriented Intelligent Monitoring of a Storage-Based Solar Photovoltaic (PV)-Powered Microgrid with Mesh Networks," Energies 2018, 11(6), 1446; doi:10.3390/en11061446. (Featured article on Energies)
- **A. Almadhor**, M. Matin and D. Gao, "Recurrent Neural Network (RNN- LSTM) Forecasting of PV Based Islanded Microgrid" *SPIE, San Diego, CA, Aug 2019.*
- **Ahmad Almadhor**, "Automatic PV Performance Diagnosis through Inverter Data using Dual Neural Network Architecture," *IEEE ROPEC, Nov'18, Ixtapa, Mexico.*
- **Ahmad Almadhor**, "Comparative Analysis of Face Detection Algorithms: Novice to Novel," *IEEE ICCAS, Oct '18, PyeongChang, S. Korea.*
- **Ahmad Almadhor**, "Deep Learning Based Face Detection Algorithm for Mobile Applications," *IEEE TENCON, Oct '18, Jeju, S. Korea.*
- **Ahmad Almadhor**, "Intelligent control mechanism in Smart Micro Grid with Mesh Networks and Virtual Power Plant Model," *IEEE CCNC, Jan'19, Las Vegas, USA.*
- M. Waseem, R. Khan, F. G., **A. Almadhor**, A. J., S. P. "An Improved Design of Supervised Differential Relay for Power Transformer with Reduced Malfunctioning," Sci.Int.,30(5),751-756,2016.
- **Ahmad Almadhor**, "Performance forecasting of distributed PV generations systems using Artificial Neural Networks (ANN) and Mesh Networks," *IEEE ICSmartGrid, Dec'18, Nagasaki, Japan.*

- **A. Almadhor**, “A Fog Computing based Smart Grid Cloud Data Security,” Int. J. Applied Info. Sys. vol. 10, no. 6. pp. 1–6, 2016.
- **A. Almadhor**, “A Survey on Generic SCADA Simulators,” Int. J. Comput. Appl., vol. 128, no. 8, pp. 38–43, 2015.

In review Papers:

- **A. Almadhor** and M. Matin “Panel Level PV performance diagnosis using DNN”, *IET Journal of electronics, Mar 2019.*
- **A. Almadhor**, M. Matin and D. Gao “A hybrid BA-PSO for Capacity Configuration Optimization in a PV system” *IEEE Access Journal, 2019.*